Nano Research
2023, 16(3): 3895–3912

ISSN 1998-0124 CN 11-5974/O4
https://doi.org/10.1007/s12274-022-4793-5

Review Article

Preparation, applications, and challenges of functional DNA nanomaterials

Lei Zhang, Mengge Chu, Cailing Ji, Jie Tan (✉), and Quan Yuan (✉)

Molecular Science and Biomedicine Laboratory (MBL), State Key Laboratory of Chemo/Biosensing and Chemometrics, College of Chemistry and Chemical Engineering, Hunan University, Changsha 410082, China

Received: 23 June 2022 / **Revised:** 15 July 2022 / **Accepted:** 18 July 2022

ABSTRACT

As a carrier of genetic information, DNA is a versatile module for fabricating nanostructures and nanodevices. Functional molecules could be integrated into DNA by precise base complementary pairing, greatly expanding the functions of DNA nanomaterials. These functions endow DNA nanomaterials with great potential in the application of biomedical field. In recent years, functional DNA nanomaterials have been rapidly investigated and perfected. There have been reviews that classified DNA nanomaterials from the perspective of functions, while this review primarily focuses on the preparation methods of functional DNA nanomaterials. This review comprehensively introduces the preparation methods of DNA nanomaterials with functions such as molecular recognition, nanozyme catalysis, drug delivery, and biomedical material templates. Then, the latest application progress of functional DNA nanomaterials is systematically reviewed. Finally, current challenges and future prospects for functional DNA nanomaterials are discussed.

KEYWORDS

DNA nanomaterial, function, preparation, biomedical application

1 Introduction

DNA, the carrier of genetic information, serves as a central component of all life on Earth [1–4]. DNA consists of four basic nucleobases, adenine (A), thymine (T), cytosine (C), and guanine (G) [5]. DNA has some unique properties, such as high precision of Watson–Crick base pairing, the high predictability of DNA helix structure, and the dynamic nature of DNA hybridization [6–10]. Based on these principles, DNA nanotechnology has been developed [11–13], enabling the design of DNA nanomaterials with desired structures and functions [14]. Due to their high designability, functional DNA nanomaterials have aroused extensive interest in biomedical fields such as biosensing and disease treatment [15–17].

After accurate design and modification, DNA nanomaterials can be endowed with unique functions [18–20]. Due to their programmability [21, 22], DNA nanomaterials of almost random sizes and shapes can be assembled by adjusting the number and order of the four nucleobases, meeting the accurate regulation requirements for biosensing [23–26]. Moreover, the surfaces of DNA nanomaterials could be precisely modified with molecular accuracy. In this way, different functional entities such as proteins [27, 28], nanoparticles [29–31], and drugs [32, 33] can be assembled with DNA to form multifunctional composite materials. These properties give hopes for DNA nanomaterials to be novel biomaterials with multiple utilities and offer promising potential for biomedical research.

In recent decades, functional DNA nanomaterials have been developed and improved rapidly [34–36]. In this review, we first elaborate on the preparation methods of DNA nanomaterials with different functions such as molecular recognition, nanozyme catalysis, drug delivery, and template for biomedical materials. Then, the latest applications of functional DNA nanomaterials in these fields are summarized. In the end, we will present the emerging challenges and perspectives of functional DNA nanomaterials, aiming to provide guidance for promoting the rapid development of DNA nanomaterials.

2 Preparation of functional DNA nanomaterials

Benefiting from the high programmability of DNA, molecules with recognition, catalysis, delivery, and therapeutic functions can be readily integrated into DNA nanomaterials, enabling the design of DNA functional nanomaterials [37, 38]. In this part, we will introduce the preparation methods of DNA nanomaterials with various structures from the perspective of function, and analyze how the structures of DNA nanomaterials match the functions.

2.1 Molecular recognition

Early detection of biomarkers has significant implications for disease diagnosis and treatment [39]. Molecular recognition of biomarkers plays an important role in accurate detection, which markedly increases sensitivity [40]. As functional DNA nanomaterials, aptamers are oligonucleotide sequences obtained by *in vitro* systematic evolution of ligands by exponential enrichment (SELEX) [41–44]. By folding into various tertiary structures, aptamers can spatially match with biological target molecules, achieving specific recognition [45, 46]. Moreover,

Address correspondence to Jie Tan, tanjie0416@hnu.edu.cn; Quan Yuan, yuanquan@whu.edu.cn

additional affinity can be imparted to natural aptamers by chemical modification [47]. This further enhanced the ability of aptamers to recognize target molecules [48]. In this part, we mainly discuss the preparation of aptamers and chemically modified aptamers for the recognition of target molecules.

Revealing the molecular-level differences between cells has instructive implications for understanding the biological mechanisms of disease. However, traditional probes for molecular recognition still have limitations in practical applications [49]. As a new type of molecular probe, aptamer can be isolated and identified by SELEX technology to differentiate specific molecular types [41]. Aptamers that recognize target cells but not control cells can be obtained by cell-SELEX. Shangguan et al. chose the leukemia cell line CCRF-CEM as the target and the B cell line Ramos as the control to select aptamers (Fig. 1) [50]. The process started with a library of 70-mer single-stranded DNA flanked by 18-mer sequences. The library was incubated with target cells and then eluted unbound DNA sequences. Subsequently, the collected DNA sequences were incubated with control cells for counterselection, and the sequences bound to the control cells were removed. After multiple rounds of selection, aptamers that specifically recognize CCRF-CEM can be enriched, and the equilibrium dissociation constants (K_d) of these aptamers were calculated to be in the nanomolar to picomolar range.

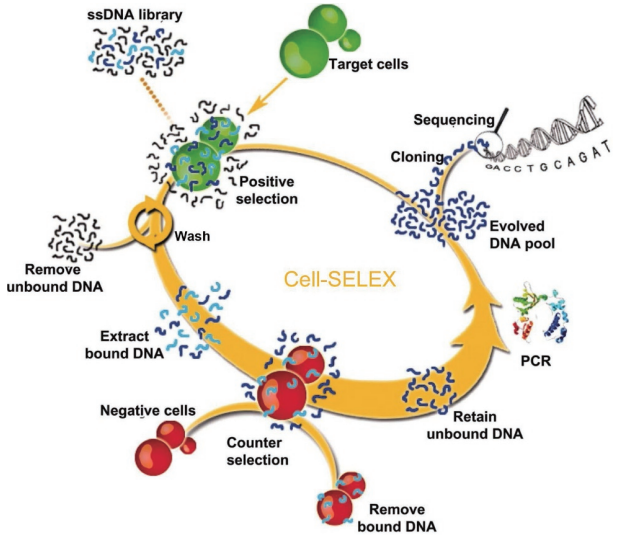

Figure 1 Representative schematic of cell-based selection of aptamers from linear single-strand libraries. Reproduced with permission from Ref. [50], © The National Academy of Sciences of the USA 2006.

For targets of interest, in addition to cells, various species such as proteins, enzymes, and peptides have been used as targets in SELEX [51, 52]. Tau protein is a microtubule-associated protein. When tau is hyperphosphorylated, it causes irreversible neurodegeneration. Teng et al. selected four tau protein fragments and their corresponding phosphorylated forms as targets for SELEX [53]. The library is 66 nucleotides long, single-stranded DNA. Protein fragment-modified Ni beads acted as targets, and the pure Ni sepharose high performance beads (Ni-TAT) were regarded as control. After 17 rounds of selection, 5 candidate sequences with strong affinity to the T231 peptide were obtained. The aptamers can be employed to recognize tau in biological fluids and reveal the pathogenesis of tau disease. At present, the novel coronavirus (SARS-CoV-2) has become a global pandemic. The receptor binding domain (RBD) of the SARS-CoV-2 spike glycoprotein has emerged as a key target for the diagnosis and treatment of SARS-CoV-2 [54]. Song et al. acquired aptamers targeting SARS-CoV-2 RBD with the help of SELEX and machine learning screening algorithm [55]. For the aptamer candidates, the authors optimized the sequence length by truncation, and the low K_d values of the optimized aptamers for RBD were 5.8 and 19.9 nM, respectively.

Compared with linear DNA, due to the lack of free ends and reduction in misfolding, circular structures show better thermal stability and improved conformational stability [56]. Combined with traditional SELEX strategies, aptamers with enhanced specific binding ability and biological stability could be obtained from circular DNA libraries. Most pseudomembranous colitis is caused by *Clostridium difficile* infection (CDI). Glutamate dehydrogenase (GDH) is highly expressed in the stools of CDI patients but not healthy individuals, making GDH a well-established biomarker for the diagnosis of CDI. Liu and colleagues attempted to select GDH targeting aptamer (Fig. 2) [57]. First, a circular DNA library was prepared by end-to-end ligation of linear DNA libraries containing 82 nucleotides. The circular library was then incubated with Ni-nitriloacetic acid (NTA) for counter-selection to remove DNA molecules bound to the Ni-beads. Unbound DNA sequences were collected to incubate with histidine-tagged recombinant GDH (rGDH)-coated Ni magnetic beads for positive selection. After 12 rounds of *in vitro* selection, the circular DNA aptamer Capt-4 with high affinity for rGDH was acquired. Based on the circular structure of Capt-4, the detection sensitivity of aptamer for GDH was significantly improved by rolling circle amplification technology. In yet another study, Mao et al. used the aptamer TBA15 targeting thrombin as the parent sequence, and added 20 random sequences and 10 primer sequences on each side to prepare linear single strands libraries [58]. Single strands were circularized by T4 ligase and isolated by polyacrylamide gel electrophoresis (PAGE) purification to prepare circular DNA libraries. Based on the magnetic bead sorting, a circular thrombin aptamer with 4-fold higher binding capacity than linear single strand aptamer was obtained after 7 rounds of selection.

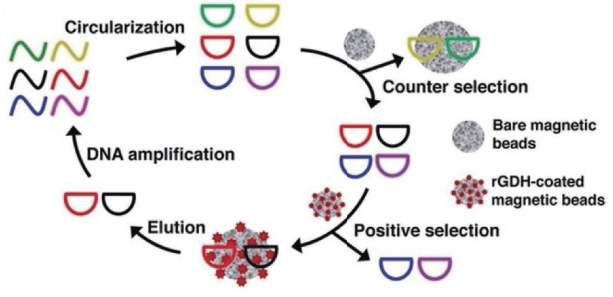

Figure 2 Representative schematic of protein-based selection of aptamers from circular single-strand libraries. Reproduced with permission from Ref. [57], © Wiley-VCH Verlag GmbH & Co. KGaA, Weinheim 2019.

The introduction of chemical modifications in nucleotides can provide novel interactions between aptamers and targets for further preparation of aptamers with strong molecular recognition ability [48]. Alterations in glycosylation have been implicated in many human diseases, and tumor-specific glycans have been investigated as potential biomarkers for cancer.Yoshikawa et al. proposed a method to generate and select aptamers with indole modifications to identify and differentiate specific protein glycosylation (Fig. 3) [59]. Specifically, water-in-oil emulsions with polymerase chain reaction (PCR) reagents were prepared to form an independent PCR reaction space, achieving efficient DNA amplification. DNA library molecules were first hybridized to magnetic beads coated with forward primers. Emulsion PCR was then performed to generate aptamer particles that each displays many copies of a single sequence. During the emulsion PCR step, the uridine nucleotide 5-[(3-indolyl) propionamide-N-allyl]-2-deoxyuridine-5-triphosphate (5-indolyl-dUTP) was directly

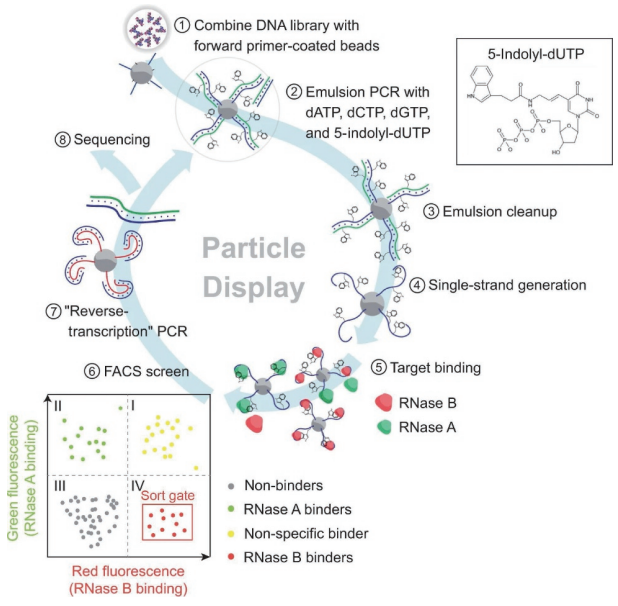

Figure 3 Representative schematic of selecting aptamers from chemically modified libraries. Reproduced with permission from Ref. [59], © Yoshikawa, A. M. et al. 2021.

incorporated as a substitute for thymidine. The incorporation of indole moiety into chemically modified bases can introduce new interactions between aptamers and glycosylated proteins, enabling highly selective recognition of protein glycan epitopes. After breaking the emulsion, the reverse strands were released via NaOH treatment, and the aptamer particles with single-stranded DNA were collected by magnetic separation. RNase A (RA) and RNase B (RB) have the same amino acid sequence, and only differ at a single N-linked glycosylation site. Fluorescently labeled RA and RB were thus used as negative controls and targets, incubating with the collected aptamer particles. Fluorescence-activated cell sorting (FACS) separated aptamer particles that generate a strong RNase B-specific signal and minimal RNase A-specific signal. After FACS, the base-modified aptamers were converted back to natural DNA templates via reverse transcription for subsequent screening. Through multiple rounds of screening and enrichment, the obtained aptamers showed selective recognition for proteins that differ only in their glycan modifications. As biomarkers of Plasmodium, there are two highly homologous lactate dehydrogenases, *Plasmodium vivax* lactate dehydrogenase (PvLDH) and *Plasmodium falciparum* lactate dehydrogenase (PfLDH). Cheung et al. reported a cubane-modified aptamer (cubamer) that can specifically recognize PvLDH and conducted an in-depth exploration of the specific binding form of the aptamer and PvLDH [60]. At first, cubane-modified deoxyuridine triphosphate (dU^{C}TP) was synthesized and the most suitable enzyme for dU^{C}TP to perform subsequent SELEX was determined. Then this library was used to perform SELEX on PvLDH bound to Ni-NTA beads. By surface plasmon resonance (SPR) test, a cubamer with an affinity for PvLDH of K_d = 670 ± 9 nM was obtained. Further, the authors demonstrated that although PvLDH and PfLDH are highly conserved and have high homology, the introduction of chemical modification of cubane increased the hydrogen bonding and hydrophobic interaction between the aptamer and PvLDH. This binding mechanism enabled cubamer to distinguish PvLDH from PfLDH.

Additionally, Tan et al. established an artificial-nucleotide-expanded screening system (ANE-SELEX) with three different chemical modifications, a ferrocenyl group, a trifluoromethyl group, and a Z:P base pair [61]. Meanwhile, various interactions such as metal chelation, hydrophobicity, and electrostatic attraction were incorporated into the SELEX process. The aptamer ZAP-1 targeting integrin α3 was screened, and it was proved that the aptamer could effectively inhibit the biological function by binding to integrin α3. In general, by means of SELEX and chemical modification, aptamers with excellent recognition properties can be prepared and optimized, providing an innovative idea for the development of DNA nanomaterial with recognition ability.

2.2 Catalysis of nanozymes

Nanozymes are a class of nanomaterials with enzymatic catalytic activity [62–64], which have the advantages of high catalytic stability, easy modification, and low preparation cost [65–67]. Biochemists have discovered that DNA, like RNA and proteins, also possesses nanozyme activity that catalyzes a range of chemical reactions [68]. In this part, we will mainly demonstrate the synthesis of DNA-based nanomaterials with nanozyme catalytic function, such as DNA enzymes (DNAzyme) and DNA-metal materials.

Copper (Cu^+)-dependent azide-alkynyl cycloaddition (CuAAC) reaction is a common click chemical reaction [69]. However, the cytotoxicity of Cu^+ limits its wide application in living systems. Liu et al. obtained the DNAzymes that can efficiently catalyze the AAC reaction at extremely low copper concentrations through SELEX (Fig. 4(a)) [70]. First, the authors synthesized an alkynyl-modified single-stranded DNA (ssDNA) library and incubated it with azide-biotin. The DNA that can catalyze CuAAC reaction was captured, isolated, amplified, and carried out to the next selection. After 25 rounds of selection, a DNAzyme called CLICK-17 with CuAAC catalytic activity was obtained. It was verified that the DNAzyme can catalyze the CuAAC reaction with low to submicromolar concentrations of Cu^+ or Cu^{2+}, and can be applied to catalyze the conjugation of various substrates such as proteins and nucleic acids. Similarly, the DNAzyme that can cleave the substrate of *Helicobacter pylori* (HP) was acquired through *in vitro* selection by Ali et al. [71]. The crude extracellular mixture of HP (CEM-HP) was utilized as the positive selection target to get DNAzyme that can cleave DNA/RNA substrates. And the CEMs of five different bacteria were employed as the counter selection target to screen out the DNAzyme that was only specifically activated by HP. Based on the excellent catalytic performance of DNAzyme, a colorimetric paper-based sensor was designed for

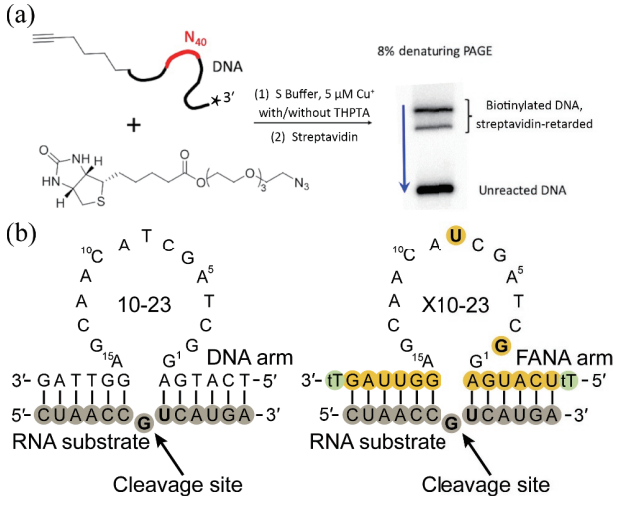

Figure 4 Preparation of DNAzyme with catalytic function by SELEX. (a) Design strategy for obtaining CuAAC-catalyzing DNAzyme by *in vitro* selection. Reproduced with permission from Ref. [70], © Liu, K. et al. 2020. (b) 10-23 and engineered X10-23 DNAzyme in complex with RNA substrates. Reproduced with permission from Ref. [72], © Wang, Y. J. et al., under exclusive licence to Springer Nature Limited 2021.

high-sensitivity and selective detection of HP.

Natural DNA enzymes exist challenges such as poor biological stability and low catalytic efficiency in practical applications. The catalytic efficiency of natural DNAzyme can be improved by new molecular design. As a classic Mg^{2+}-dependent RNA cleaving enzyme, 10-23 DNAzyme has similar problems. Wang et al. modified 10-23 DNAzyme with xeno-nucleic acids (XNAs) and thus developed a new X10-23 DNAzyme (Fig. 4(b)) [72]. 2'-Fluoroarabino nucleic acid (FANA, an XNA) replaced the DNA residues in the substrate recognition domain and catalytic core of the classical 10-23 DNAzyme. And then threose nucleic acid (TNA) was added to both ends of the DNAzyme. The introduction of FANA and TNA increased the stability of X10-23 without affecting the catalytic performance of the enzyme. The modified X10-23 can improve the activity and stability of DNAzyme, leading to new research and strategies of DNAzyme for future clinical application.

In addition to natural DNAzymes, metal nanoparticle-based DNA artificial enzymes (nanozymes) also possess unique catalytic properties. Plasmonic metal nanoparticles can convert absorbed photons into heat, and this photothermal property has been applied to boost the activity of enzymes. To obtain highly active nanozymes, Wei et al. synthesized novel nanoflower-like gold nanostructures (AuNFs) by a one-pot metallization technique using diblock DNA as a scaffold (Fig. 5(a)) [73]. The DNA scaffold consists of two parts, polyadenine helps to form the nanoflower-like structure and aptamer enables the nanozyme with recognition ability for cancer cells. AuNFs have peroxidase-mimicking activity, and their activity was tested by the hydrogen peroxide-o-phenylenediamine (H_2O_2-OPD) system. The number of cancer cells was quantified by observing the color change of the solution catalyzed by the nanozyme. Compared with spherical gold nanostructures (AuNSs), the AuNFs exhibited higher selectivity and catalytic activity for tumor cells. Similarly, Li et al. also developed a DNA-directed assembly method to combine two diameters of gold nanoparticles (AuNPs) to fabricate halo-like gold nanostructures (nanohalo) [74]. First, 50 nm plasmonic large gold nanoparticles (L-AuNPs) and 13 nm catalytically active small gold nanoparticles (S-AuNPs) were synthesized. The surfaces of L- and S-AuNPs were modified with two thiolated DNA complementary sequences, respectively. By means of complementary base pairing, the two AuNPs were linked into a nanohalo. Adjusting the length and density of DNA sequences can alter the distance of AuNPs and the catalytic activity of nanohalo. The catalytic reaction that takes place on S-AuNPs changed the dielectric constant, resulting in a dramatic change in the plasmonic resonance of the nanohalo. Therefore, monitoring the plasmonic resonance of nanohalo can provide quantitative information on nanocatalysis.

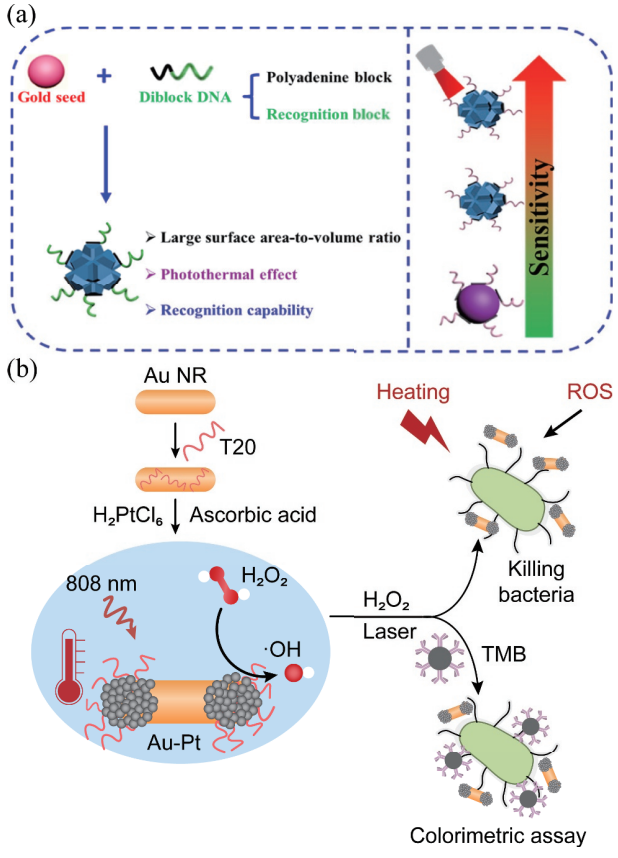

Figure 5 DNA-based composites with enzyme catalysis were prepared by coupling DNA with metal nanoparticles. (a) Schematic illustration of diblock DNA-guided one-pot fabrication of nanoflower-shaped nanozymes. Reproduced with permission from Ref. [73], © American Chemical Society 2021. (b) Schematic illustration of DNA-directed Au-Pt bimetallic nanoparticles with enhanced enzyme-like catalytic activity for detection and elimination of Escherichia coli. Reproduced with permission from Ref. [76], © Elsevier B.V. 2021.

DNA-mediated nanozyme exhibits excellent catalyst activity. However, most previous research involving DNA as ligands has only involved monometallic particles [75]. Bimetallic nanoparticles containing Au and Pt have sparked widespread interest owing to their multifunctional and synergistic catalytic properties. Lu et al. synthesized dumbbell-shaped Au-Pt bimetallic nanozymes for the first-time using DNA-encoded seed growth method, and investigated the mechanism by which DNA sequences regulate the growth of bimetallic nanoparticles (Fig. 5(b)) [76]. First, Au nanorods (Au NRs) were synthesized by silver ion-assisted method, and then the Au NRs were respectively incubated with solutions containing 20 A, C, or T deoxyribonucleotides. Followed by the addition of chloroplatinic acid (H_2PtCl_6) as the Pt precursors. The research suggested that only T20 is more inclined to form dumbbell-like Au-Pt bimetallic structures. The T20 DNA sequence provided interaction between Au and Pt, inducing the codable deposition of Pt, resulting in the formation of dumbbell-shaped Au-Pt nanoparticle enzymes. To investigate the catalytic activity of Au-Pt nanoparticles, experiments were performed using tetramethyl benzidine (TMB) as a substrate in the existence of H_2O_2. The oxidation peak of TMB increased significantly due to the synergistic effect of gold and Pt, illustrating that the prepared DNA-mediated Au-Pt nanoparticles exhibit strong nanozyme catalytic activity.

2.3 Drug delivery

To safely and efficiently deliver drugs to cells, the vehicle must be made from materials that do not cause damage to biological systems [77]. Then, the vehicle needs to provide enough adsorption sites and space to carry the drug with high loading [78–80]. Functional DNA nanomaterials have advantages such as good biocompatibility and designability, and have proven to be an attractive drug delivery platform in recent years [33, 81, 82]. DNA vehicles with different structures have been developed based on complementary base pairing, and hydrophilic and hydrophobic interactions [83, 84]. This section mainly introduces DNA nanocarriers such as DNA hydrogels, polyhedrons, and nanotubes.

DNA hydrogel is a three-dimensional network polymer material formed by physical or chemical cross-linking [85, 86]. In hydrogels, water is usually employed as the solvent and macromolecules as the solute. The composition and structural characteristics endow the hydrogel with high biocompatibility, low toxicity, and good flexibility. Thus, hydrogel is considered as an

ideal drug vehicle. Zhang et al. designed a DNA hydrogel loaded with the antitumor drug camptothecin (CPT) [87]. They first modified the three-component DNA strands with phosphorothioate to provide sites for CPT binding. Subsequently, the carboethyl bromide-modified CPT was successfully grafted onto the DNA strands. The DNA strands were mixed to self-assemble into two kinds of Y-shaped building blocks, Y-1 motif and Y-2 motif. Notably, the introduction of CPT on the DNA backbone did not affect the Watson–Crick base pairing and assembly properties of the DNA strands. Finally, physical hydrogel was assembled through the sticky ends of the two kinds of Y-shaped motifs (Fig. 6(a)). The drug-loaded hydrogel can be injected into the disease site and exhibits excellent long-term cytotoxicity against cancer cells.

DNA hydrogels that are stable under extremely acidic pH conditions have rarely been reported, posing challenges for practical drug delivery applications. Hu et al. formed acid-resistant and pH-responsive DNA hydrogels by radical polymerization of two A- or C-rich oligonucleotides and acrylamide monomers (Fig. 6(b)) [88]. When pH < 3.0, A-rich sequences formed double-stranded and parallel A-motif structures through reverse Hoogsteen base pairing and electrostatic force. In the pH range of 4.0–6.0, the C-rich sequence formed a quadruplex half i-motif by reverse Hoogsteen base pairing. Therefore, at acidic pH (1.2–6.0), A-motif or i-motif acted as hydrogel bridging units, making the DNA nanomaterial exhibit a hydrogel state. Under neutral conditions, the deprotonation of the A and C bases led to the dissociation of A-motif and i-motif structures into single strands, thus the DNA hydrogel became a solution state. This DNA hydrogel, which switches between gel and solution states in response to pH changes, will be suitable for drug delivery in different pH environments. The authors chose insulin as a model drug and encapsulated it in a pH-responsive hydrogel, and subsequently transferred to solutions simulating the gastrointestinal (GI) tract environment, including artificial gastric fluid (AGF, pH 1.2), artificial duodenal fluid (ADF, pH 5.0), or artificial intestinal fluid (AIF, pH 7.2). The insulin@DNA hydrogel composite can effectively protect insulin through low-acidity environments such as the stomach and achieve efficient insulin release in the small intestine. Spherical nanogels for the delivery of small interfering RNA (siRNA) were constructed by Ding and colleagues using two building blocks [89]. In this work, DNA-polymer brushes with abundant cross-linking sites were first prepared by covalently linking dibenzocyclooctyl-modified DNA strands with azide-modified polycaprolactone via a click reaction. A central functional double-stranded siRNA and two overhang single-stranded DNA sequences were contained in siRNA linkers. Two building blocks, DNA-polymer brushes and siRNA linkers, were mixed in solution to rapidly assemble into size-tunable nanogels. This work provided a powerful strategy for efficient siRNA delivery.

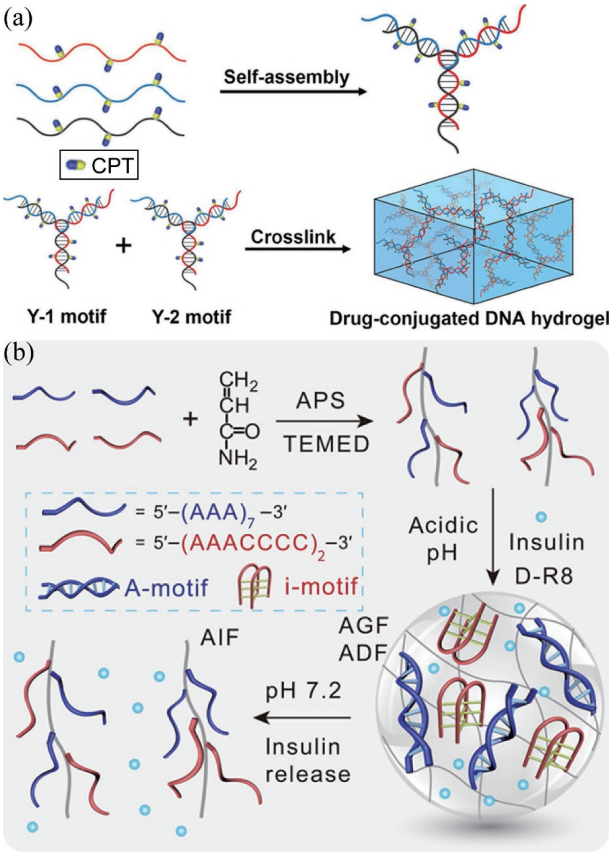

Figure 6 Construction of DNA hydrogels for drug loading. (a) Schematic diagram of the synthetic route of the CPT-loaded physically cross-linked DNA hydrogel. Reproduced with permission from Ref. [87], © American Chemical Society 2020. (b) Schematic diagram of preparation of insulin-loaded pH-responsive chemically cross-linked DNA hydrogels. Reproduced with permission from Ref. [88], © American Chemical Society 2022.

Such a drug delivery strategy is not only applicable to DNA hydrogels but also to DNA polyhedral structures. Zhang and coworkers did elegant work in designing drug-grafted DNA tetrahedrons (TET) [90]. They first introduced carbonylethyl bromide on the model drug CPT, which was then covalently linked to phosphorothioate (PS)-modified DNA. The DNA sequences of the four grafted CPTs obtained are partially complementary, and then self-assemble to form a drug-containing DNA tetrahedron. Ingeniously, by precisely adjusting the number and position of PS, the drug loading of CPT can be controlled. This is of great help for improving the hydrophilicity and antitumor efficacy of DNA-drug conjugates. Besides, Xiao et al. assembled another DNA tetrahedron containing four single strands [91]. The vertex of one of the single strands is coupled to the AS1411 aptamer to target tumor cells, and the vertex of the other chain is attached to the sticky end. The siRNA that inhibits melanoma Braf gene was linked via sticky ends of the tetrahedron, achieving the efficient load of siRNA. Cellular experiments demonstrated that the siRNA-loaded DNA tetrahedron showed obvious Braf gene silencing compared to other controls. Recently, Fu et al. designed the tetrahedral framework (TDF) nucleic acids for the delivery of double-stranded siRNA by a similar strategy [92]. The delicately designed overhang sequences in the tetrahedron were linked to the overhang ends of the siRNA double strands, enabling the effective loading of the siRNA therapeutic agent in the tetrahedron. After entering cells, siRNA can inhibit the expression of C-C chemokine receptor 2 gene and protein in cells, and alleviate the damage to motor nerve function in intracranial hemorrhage mice.

Wang et al. designed DNA octahedral wireframes for the delivery of cambrastatin (CA4), a broad-spectrum microtubule inhibitor [93]. The authors first prepared the CA4 phosphoramidite group, and then modularly synthesized CA4-functionalized Sgc8 aptamer (CA4-FS) by connecting with four natural bases by solid-phase synthesis. Among them, Sgc8 aptamer was used to target tumor cells. Based on the hierarchical self-assembly strategy, six four-way-connected DNA tiles were used as the vertices of a DNA octahedron, and the single-stranded domains of the tiles were connected to form a DNA octahedron wireframe. The two single strands dangling from the edge of each DNA wireframe can be precisely paired with CA4-FS, resulting in the final formation of 24 CA4-functionalized DNA nanocore-shell structures (Fig. 7(a)). Controllable drug loading and release can be achieved through this modular precision design.

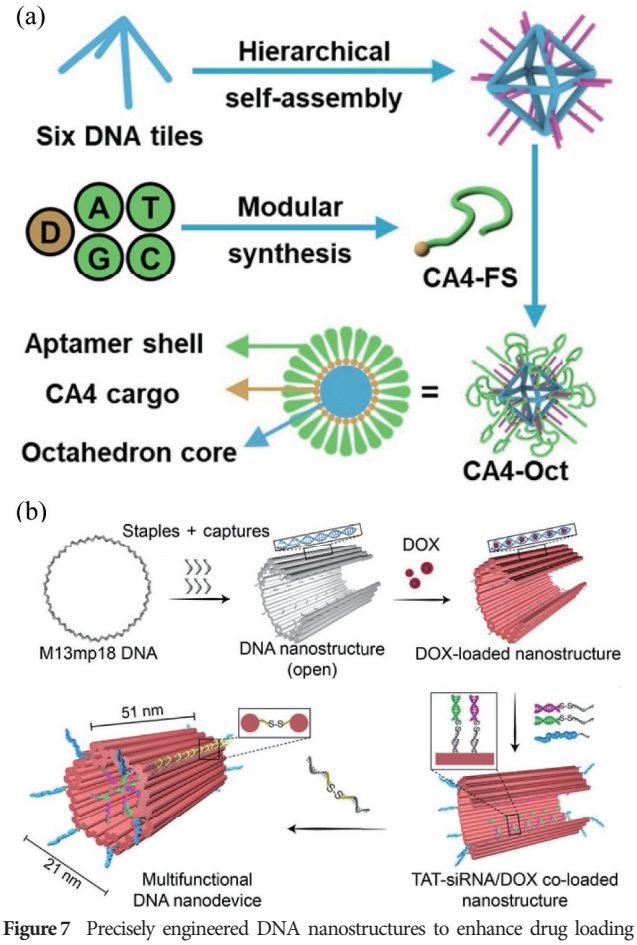

Figure 7 Precisely engineered DNA nanostructures to enhance drug loading efficiency. (a) DNA octahedral wireframe enhances CA4-FS delivery for targeted therapy. Reproduced with permission from Ref. [93], © American Chemical Society 2020. (b) Construction of siRNA/DOX co-loaded DNA nanotubes for synergistic therapy. Reproduced with permission from Ref. [94], © Wiley-VCH GmbH 2020.

Wang and coworkers proposed a novel formulation to develop nanotubes for co-loading of siRNA therapeutics and chemotherapeutic drug doxorubicin (DOX) [94]. They fabricated hollow nanostructures by assembling a single M13 phage genomic DNA strand and multiple short strands. DOX was inserted into DNA nanostructures based on hydrophobic interactions. To load two types of siRNA, 48 capture strands were attached to the inner surface of the DNA nanotube at designated positions. The transmembrane peptide TAT, which enhances cellular uptake and tumor accumulation, was then incorporated into the DNA origami. Finally, a tubular DNA nanodevice with a length of 51 nm and a diameter of 21 nm was constructed by hybridizing the predesigned locked strands with the edge of the DNA origami (Fig. 7(b)). At the tumor site, the tubular DNA nanodevice reacted with glutathione to cause locked strand breaks, allowing the controlled release of siRNA for synergistic tumor therapy.

Zhang et al. reported a strategy to manipulate the drug delivery capacity of DNA nanoflowers by incorporating ferrocene base into DNA strands [95]. Specifically, they designed DNA templates that contain complementary sequences of DNA-ferrocene, complementary sequences of aptamers, and primers. The DNA nanoflowers were then assembled from long DNA building blocks generated by rolling circle replication. Due to the introduction of ferrocene bases, the nanoflowers possessed Fenton reaction-induced self-degradability. In the xenograft tumor model, the nanoflowers loaded with doxorubicin could efficiently deliver their cargos to tumors, significantly improving the therapeutic efficacy of doxorubicin. De Vries and colleagues designed DNA nanomicelles for ophthalmic drug delivery. This nanomicellar carrier can prolong the survival time of drugs on the eye surface [96]. The authors synthesized DNA strands using dodecyne-modified 2'-deoxyuridine nucleotides to impart hydrophobic properties. When introduced into an aqueous environment, DNA amphiphiles self-assembled into micellar nanoparticles. Subsequently, antibiotic-loaded nanomicelles were formed by hybridizing with kanamycin B-binding DNA aptamers and neomycin B-binding RNA aptamers. The drug-loaded nanomicelles adhered for few hours to the cornea and therefore dramatically increased the adherence time of the drug cargo, improving the therapeutic efficacy of drugs.

2.4 Templates for biomedical materials

Studies have shown that DNA nanomaterials with specific shapes are utilized as templates for the controllable preparation of inorganic non-metallic and polymer nanomaterials [97–99]. For example, DNA origami techniques allow these materials to be tailored in distinct patterns, endowing the newly synthesized materials with unique functionalities [100–102]. DNA templates can either be removed after the controlled synthesis of new materials [7, 103] or become part of the reaction products [104, 105]. This provides an essential idea for the preparation of biomedical materials. In this section, we will summarize the controllable synthesis of functional nanomaterials using DNA origami as a template.

As a vital component of teeth, natural hydroxyapatite (HAP) has great biological activity and osteoconductivity [106]. However, existing artificial HAP biomaterials suffer from low mechanical stiffness and toughness, limiting their application in the biomedical field. To overcome this problem, Zhou et al. fabricated DNA-HAP composites with high mechanical stiffness and toughness based on the DNA template (Fig. 8(a)) [107]. Under electrostatic interactions, rigid double-stranded DNA was coupled with cationic surfactants containing flexible alkyl chains to form templates for electrospun DNA fibers and films. The large specific surface area of the template offered a number of nucleation sites for the mineralization of HAP, and thus long-range and high-stiffness DNA-HAP composites were successfully prepared. This strategy realized the long-range ordered HAP preparation guided by DNA templates, which provides a promising material for the preparation of dental inlays. Wu and colleagues also chose DNA origami with specific forms as a template to guide the mineralization of CaP nanocrystals [108]. The phosphate group of DNA has a high affinity for calcium ions, thus DNA origami structure can induce the nucleation of CaP crystals in a metastable CaP supersaturated solution, effectively controlling the mineralization process of CaP. By optimizing conditions such as supersaturation, temperature, and time, CaP nanoclusters can customize uniformly on the DNA origami surface according to the template. Moreover, the CaP crystal itself has excellent thermal stability, and the mineralization of CaP helps to improve the thermal stability of DNA nanostructures. In conclusion, using DNA nanomaterials as templates can precisely control the assembly of inorganic non-metallic materials and achieve fine morphological regulation. Correspondingly, the formation of new materials also endows DNA nanostructures with new functions.

Polydopamine (PD) is a biosynthetic polymer with good biocompatibility and superior adhesion properties, which has been studied in the fields of biomaterial surface modification and adhesion. Due to the complex structure and synthesis process of PD, controllable synthesis of PD with precise morphology is still difficult. The DNA origami template strategy was applied to the

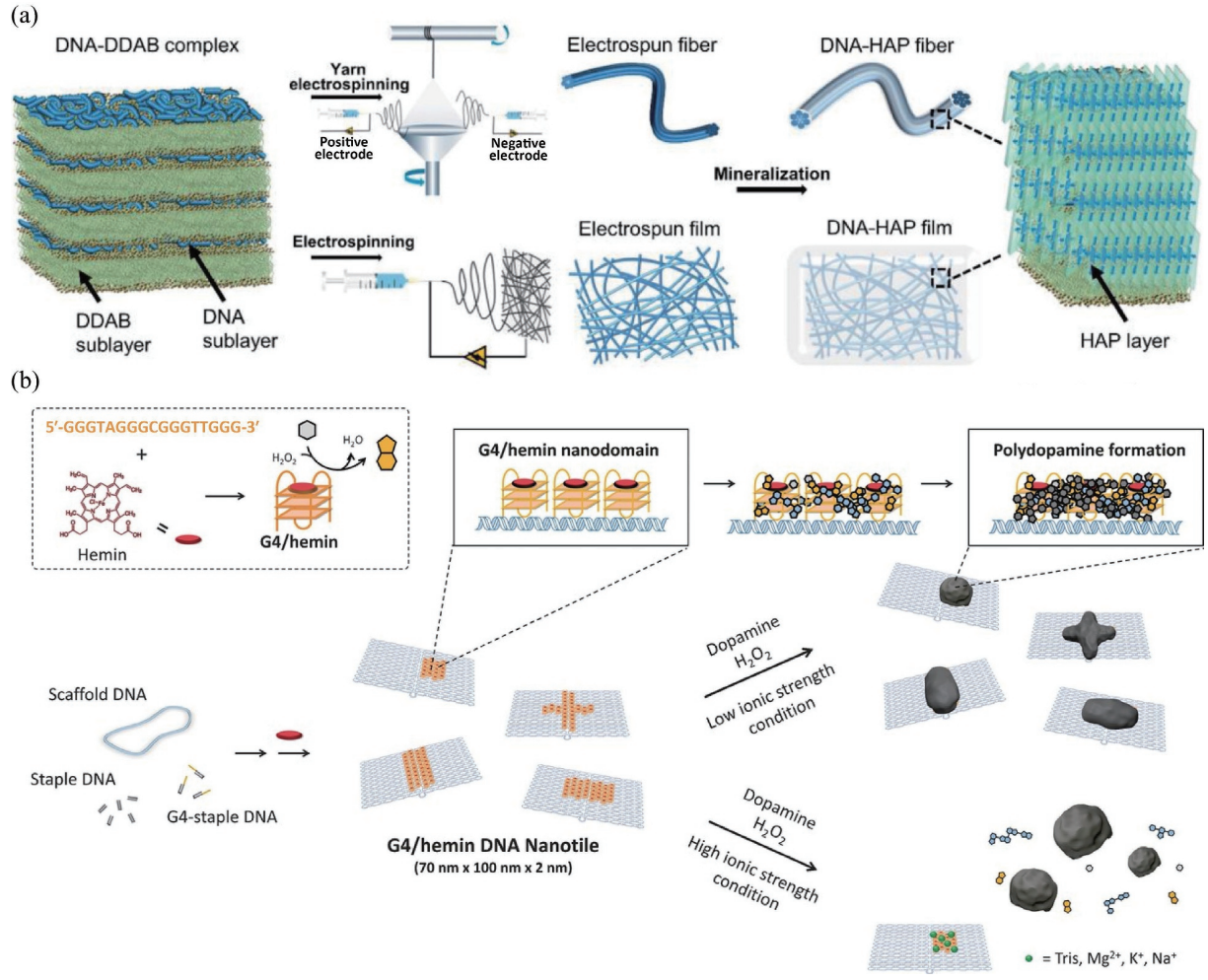

Figure 8 DNA as a template for the synthesis of inorganic nanomaterials and polymers. (a) Schematic of the preparation of DNA-HAP fibers and films using DNA sublayer as a template. Reproduced with permission from Ref. [107], © Wiley-VCH GmbH 2022. (b) Schematic of the fabrication of well-defined PDs on DNA nanosheets. Reproduced with permission from Ref. [109], © Tokura, Y. et al. 2018.

polymerization of dopamine to PD by Tocura et al. (Fig. 8(b)) [109]. A G4 reaction center was introduced on DNA origami, and heme was embedded in the G4 center. Heme has peroxidase activity, which can oxidize dopamine and accelerate the polymerization of dopamine. Dopamine will only polymerize and form PD in a specific shape at the G4-hemin-modified region. Furthermore, under acidic conditions, the resulting PD nanostructures can be easily separated from DNA origami templates. Winterwerber et al. arranged G4 strands embedded with the photosensitizer protoporphyrin IX (PPIX) in a specified pattern on DNA origami [110]. Under light conditions, the photosensitizer PPIX in the G4 sequence was able to generate reactive oxygen and further initiated the oxidative polymerization of dopamine, resulting in polydopamine-DNA hybrid materials with well-defined nanoscale dimensions. These strategies provided a pathway for the controlled synthesis of PD commonly used in advanced biochips and sensors.

Great efforts have been devoted to applying DNA nanomaterials as scaffolds to control the assembly of vesicles. Using circular DNA origami as an external backbone template, Yang et al. assemble lipid molecules on the inner surface of DNA origami [111]. First, scaffolds containing 8,064 nucleotides and multiple short strands were mixed and self-assembled into circular DNA structures through an annealing reaction. Each circular DNA was internally functionalized with 16 evenly distributed DNA strands. Specifically, the extended strand within the ring was coupled with the 1,2-dioleoyl-glycerol derived lipid chain by thiol-maleimide hybridization, followed by dialysis to remove detergents for mediating lipids assembly. By precisely adjusting the size of the DNA rings, the authors controlled the synthesis of highly dispersed liposome vesicles with dimensions of 29, 46, 60, and 94 nm (Fig. 9(a)). Furthermore, Zhang and colleagues designed DNA nanocages as external scaffold templates to guide liposome assembly into the same form as the nanocages [112]. The properties of the internally synthesized liposomes can be tuned by adjusting the size of the nanocages, as well as the amount and location of DNA extended within the cages.

In contrast to the above-mentioned methods, vesicles can also be shaped using DNA nanomaterial as endoskeletons. For example, Perrault et al. designed a wire-framed octahedron with 48 extended short chain handles based on DNA origami (Fig. 9(b)) [113]. The handles were hybridized to the DNA strands conjugated to 1,2-O-dioctadecyl-glycerol in a surfactant solution. By dialysis, the surfactant is selectively removed, resulting in the formation of a fused lipid bilayer around the DNA octahedron. From the transmission electron microscopy images, it can be observed that the surface of the DNA octahedron is covered with a layer of film, indicating the successful preparation of liposomes.By applying a similar approach, Kurokawa fabricated DNA gel shell-supported liposomes via electrostatic interactions between negatively charged DNA and positively charged lipid 1,2-dioleyl-3-trimethylaminopropane (DOTAP) droplets [114]. This approach facilitated the expansion of DNA-liposome hybrid systems. In conclusion, by adjusting the structure of DNA templates, the construction of vesicles of different shapes and compositions can be achieved.

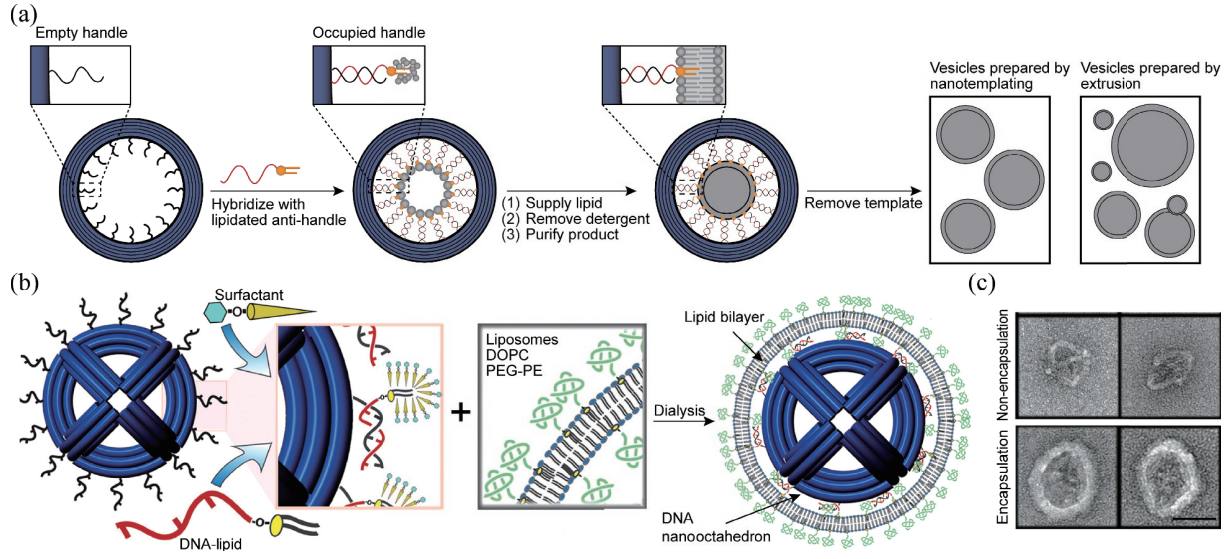

Figure 9 DNA as a template to generate liposomes. (a) Using DNA origami ring as outer skeleton template, liposomes with controllable size were generated internally. Reproduced with permission from Ref. [111], © Macmillan Publishers Limited 2016. (b) The DNA nano-octahedron acts as an endoskeleton on which to grow liposomes. (c) Transmission electron microscopy images of non-encapsulated and encapsulated DNA octahedra. Scale bar 50 nm. Reproduced with permission from Ref. [113], © American Chemical Society 2014.

3 Biomedical application

Based on the high designability of DNA, DNA nanomaterials with diverse sizes and geometries have been fabricated and dedicated to biomedical fields [24, 115, 116]. By combining various functional molecules, DNA nanomaterials could be designed with high sensitivity, high loading capacity, and anti-degradation ability [117–119]. These unique properties equip DNA nanomaterials with great application potential in the biomedical field. In this part, we mainly outline the state-of-the-art applications of functional DNA nanomaterials in biosensing, bioimaging, drug delivery, and disease treatment.

3.1 Biosensing

Recently, nucleic acid-based biosensing strategies have received increasing attention in basic and clinical research in the biomedical field [120–124]. Owing to their precise identification capabilities, DNA nanomaterials have been used to detect target DNA/RNA for the diagnosis of bacterial infection or cancer [125–131]. At the same time, various rapid and high-precision detection methods have been proposed, and the analytes have been expanded to small molecules, proteins, and so on [132–136]. We systematically summarize functional DNA nanomaterials for recognizing and biosensing of nucleic acids, ions, small molecules, and proteins in this section.

Control of the COVID-19 pandemic requires precise and easy-to-operate tests to identify infected individuals rapidly. DNA nanotechnology has shown significant advantages in the construction of SARS-CoV-2 nucleic acid sensors. Recently, Wang et al. developed a tetrahedral DNA-functionalized field-effect transistor (FET) sensor for highly sensitive detection of SARS-CoV-2 [137]. Tetrahedral DNA nanostructures were constructed by one-step self-assembly, consisting of a rigid tetrahedral base and a flexible arm. The arm included a probe for recognizing SARS-CoV-2 nucleic acid. The three vertices at the bottom of the tetrahedron were decorated with amino base groups, which was convenient for fixing the tetrahedron on the FET. The tetrahedral structure enabled efficient recognition and signal transduction of SARS-CoV-2 nucleic acid. Without nucleic acid extraction and amplification, the average diagnostic time of the sensor was about 80 s, and the detection limit can approach 1 or 2 copies per 100 μL of clinical samples. Based on the above study, Wu et al. immobilized three-probe DNA TDFs on graphene to fabricate FET ultrasensitive sensors [138]. This further improved the capture efficiency and recognition performance of SARS-CoV-2 nucleic acid. The triple recognition probes target the ORF1ab gene, RdRp gene, and E gene region of the SARS-CoV-2 RNA region, respectively. Compared with ssDNA probes, TDF dimers efficiently prevent probes from intertwining and nonspecific adsorption on graphene substrates. The synergy of the three probes and the special dimer nanostructure imparted the sensor with higher affinity, selectivity, and responsiveness. The V_{Dirac} of TDF dimer device exhibited a significant shift when a small amount of target RNA was added, demonstrating the high sensitivity of the sensor.

Messenger RNAs (mRNAs) are single-stranded RNAs that mediate the transfer of genetic information from the cell nucleus to ribosomes in the cytoplasm, where they serve as a template for protein synthesis [139]. Precise detection of tumor-related mRNA in living cells facilitates in-depth tumor research. He et al. designed a DNA tetrahedron nanotweezer (DTNT) composed of four specialized DNA single strands [140]. The nanotweezer contained two aptamers that modify Cy3 and Cy5 fluorophores, respectively. The aptamers approached each other after binding to the target mRNA, promoting fluorescence resonance energy transfer (FRET) between Cy3 and Cy5 (Fig. 10(a)). As depicted in Fig. 10(b), quantitative detection of mRNA can be achieved by monitoring ratiometric fluorescence in FRET. As the concentration of target mRNA increased from 0 to 50 nM, the fluorescence intensity of DTNT decreased rapidly at 565 nm and increased at 662 nm. The FRET signal increased almost 9-fold, indicating that the DTNT could efficiently identify the target mRNA. MicroRNAs (miRNAs) are small endogenous RNAs that play important roles in posttranscriptional gene regulation [141–143]. In a similar study, multicolor-encoded DNA tetrahedron was prepared by Zhou et al. for simultaneous detection of two types of miRNA in living cells [144]. Compared with free probes, this design was more resistant to nucleases, providing an idea for the simultaneous stable detection of multiple miRNAs.

DNA-based nanodevices can usually be activated by ions and molecules such as hydrogen ions and ATP, with the potential to precisely detect these ions and molecules. pH is a substantial environmental factor in tumorigenesis, and early detection of

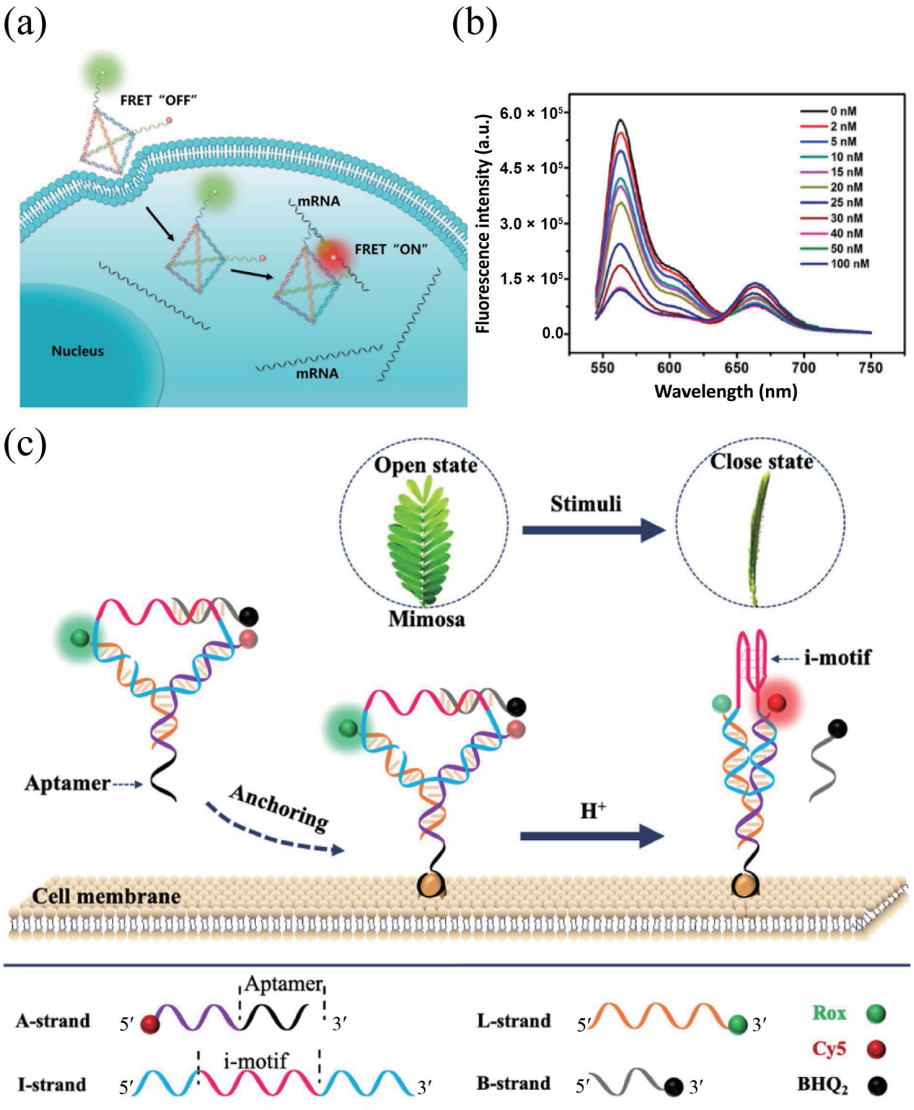

Figure 10 Detection of nucleic acids and small molecules through functional DNA nanomaterials. (a) Mechanism of DTNT nanoprobes for tumor-associated mRNAs. (b) Fluorescence spectral response of DTNT to target mRNA in different concentrations. Reproduced with permission from Ref. [140], © American Chemical Society 2017. (c) Principle of DNM for precise sensing of extracellular pHe. Reproduced with permission from Ref. [145], © American Chemical Society 2020.

extracellular pH (pHe) has a guiding role in tumor diagnosis. Encouraged by the stimuli-responsive behavior of mimosa, Chen et al. fabricated a DNA nanosensor (DNA nanomimosa, denoted as DNM) for ratiometric sensing pHe of tumor (Fig. 10(c)) [145]. The DNM was composed of 4 single-stranded DNA strands, A-strand, B-strand, L-strand, and I-strand. The A strand labeled with Cy5 contains the AS1411 aptamer for anchoring tumor cells. The I-strand contains an i-motif that responds specifically to pH. Additionally, the L and B strands were separately labeled with carboxy-x-rhodamine (Rox) and carboxy-x-rhodamine (BHQ2). At neutral pH, the DNA nanostructures remained in the Y-shape, that is the "open" state. Meanwhile, Cy5 undergoes FRET with neighboring BHQ2, thus Rox displayed a strong signal. When encountering target tumor cells, DNM could anchor on the tumor cell surface. Subsequently, the lower pH in the tumor microenvironment stimulated the i-motif to form the quadruple-helix structure, resulting in a structural change in the DNM and energy transfer from Rox to Cy5. Thus, pH sensing can be achieved by monitoring the FRET ratio (Cy5/Rox). The authors demonstrated this conclusion, with a gradual increase in FRET efficiency with decreasing pH value. Studies have shown that DNM has excellent specificity, enabling high-resolution pH sensing.

To detect ATP molecule in living cells, Zhao et al. constructed a DNA nanodevice containing two components, an ATP-targeting aptamer and an upconverting nanoparticle [146]. Initially, the aptamer was bound to complementary DNA strand containing a photocleavable group, placing the aptamer in a locked state. Under light irradiation, the photocleavable group was cleaved, and the affinity of aptamer with the complementary DNA strand decreased. When the target ATP was present, ATP was readily bound to the aptamer in the open state. In this way, the aptamer with the fluorescent group separated from the complementary strand with the quencher, thereby realizing the sensing of ATP by the fluorescent signal. The experimental results showed that the DNA nanodevice can realize ATP sensing with high sensitivity and selectivity.

DNA nanosensors could also be utilized to the sensing of protein in subcellular organelles. Based on previous work, Shao et al. proposed an organelle-specific light-activated nanosensor for selective and precise imaging of human apurinic/apyrimidinic endonuclease 1 activity in mitochondria and nucleus [147]. The sensor platform was designed by light-activated DNA fluorescent probes, upconversion nanoparticles, and specific organelle localization structures. Controlled localization and near-infrared (NIR) light-mediated *in situ* activation enable the sensor to

specifically profile enzyme activity at the subcellular level. In another study, the NO produced by nitric oxide synthase 3 (NOS3) participates in driving key signaling pathways, thus monitoring NOS3 activity has crucial implications. By integrating a diaminorhodamine (DAR) fluorophore that specifically responds to NO, a recognition group targeting the plasma membrane or trans-Golgi network (TGN), and an internal reference dye for ratiometric detection, Jani et al. constructed fluorescent DNA probes that can quantitatively sense NOS3 activity [148]. The NOS3 enzymatic activity was monitored by detecting the ratio of the luminescence intensity of the DAR dye and the reference dye by fluorescence microscopy. It was found that NOS3 on the plasma membrane was highly active. While NOS3 on the TGN was inactive, it is critical for the integrity of the Golgi. The above results indicated that the biosensors based on DNA nanomaterials offered an idea for monitoring enzymatic activity in subcellular structures, and can be used to explore the relationship between enzymatic function and cellular structure.

3.2 Bioimaging

Accurate imaging of diseased tissue is a prerequisite for diagnosis and treatment [149]. DNA molecules have the ability of molecular recognition, which has great potential in precise imaging [150]. DNA nanomaterials allow the incorporation of fluorescent dyes, quantum dots (QDs), and other imaging tags into DNA nanostructures through covalent or non-covalent interactions [151–153]. This fact makes DNA nanostructures of great utility in imaging applications. Over the past decades, functional DNA nanomaterials have been elaborated for bioimaging.

As one of the most commonly used labels for cell imaging, fluorescent dyes can be facilely modified on DNA nanomaterials. In recent years, functional DNA nanomaterials modified with fluorescent dyes have been generated. For example, Zhong et al. proposed DNA octahedral fluorescent probes for imaging of two tumor-associated mRNAs, GalNAc-T mRNA and TK1 mRNA (Fig. 11(a)) [154]. The DNA octahedron consists of 8 DNA strands, which are the mRNA aptamers modified with quencher, the nucleic acid strands modified with Cy3 or Cy5 fluorophore, and the AS1411 aptamer for enhanced probe internalization. In the presence of the target mRNA, the quencher-labeled aptamer bound to the target mRNA, resulting in the dissociation of the aptamer from the DNA octahedral backbone and the recovery of the fluorescent signal. In addition, the AS1411 aptamer promoted the internalization of octahedral probes into cancer cells to image intracellular mRNA. The nanoprobe can detect two targets simultaneously, which provides a new idea for multiplex detection of tumor biomarkers based on DNA nanomaterials. Xiao et al. co-assembled DNA block copolymers (PS-b-DNA) and NIR-II dyes into spherical nucleic acid (SNA) micelles for non-invasive imaging of brain tumors [155]. The dyes were loaded into the hydrophobic core inside the SNA in a controllable manner, significantly improving the delivery efficiency of the dyes. Experiment results displayed that the fluorescence intensity of the glioblastoma site after injection of PS-b-DNA was about 4 times higher than that of PS-b-PEG loading the same dye. SNAs with multivalent structures had high affinity to cell membrane-bound scavenger receptors, ensuring that the loading dyes can effectively penetrate the blood–brain barrier for successful diagnostic imaging of glioblastoma.

Taking advantage of the unique optical properties of QDs with the programmability of DNA nanomaterial, the prepared QDs-modified DNA fluorescent probes have good potential in biological imaging [156]. Ma et al. coupled the quencher-modified DNA with CdTe:Zn^{2+} QDs to prepare nanobeacon for labeling and detection of low-abundance nucleic acids in living cells [157]. In the absence of HIV-1 genomic RNA, the fluorescence of the QD nanobeacon was quenched by the quencher. When the target sequence was present, the target sequence hybridized with the hairpin DNA, and the fluorescence of QDs turned on. Therefore, this QD-based nanobeacon could be applied to image single RNAs in living cells. The combined design of DNA nanomaterials and QDs can be applied not only to the biological imaging of nucleic acids, but also the proteins. Combining QDs and DNA, Zhou et al. developed a highly sensitive technique for imaging multiple endogenous proteins in cells (Fig. 11(b)) [158]. Cells are first incubated with a series of primary antibodies labeled with specific oligonucleotide sequences that bind to multiple targets in the cells. The oligonucleotide sequences on the primary antibodies not only served as barcodes for each antibody, but also used as anchors for the immobilization of orthogonal ssDNA linkers. Then, by simply mixing biotinylated oligonucleotides with streptavidin-modified QDs, long tandem hybrids can be prepared and signal amplified for imaging. Simultaneous application of 5–10 color QDs in each hybridization cycle enables fast and sensitive immunostaining. Compared to traditional

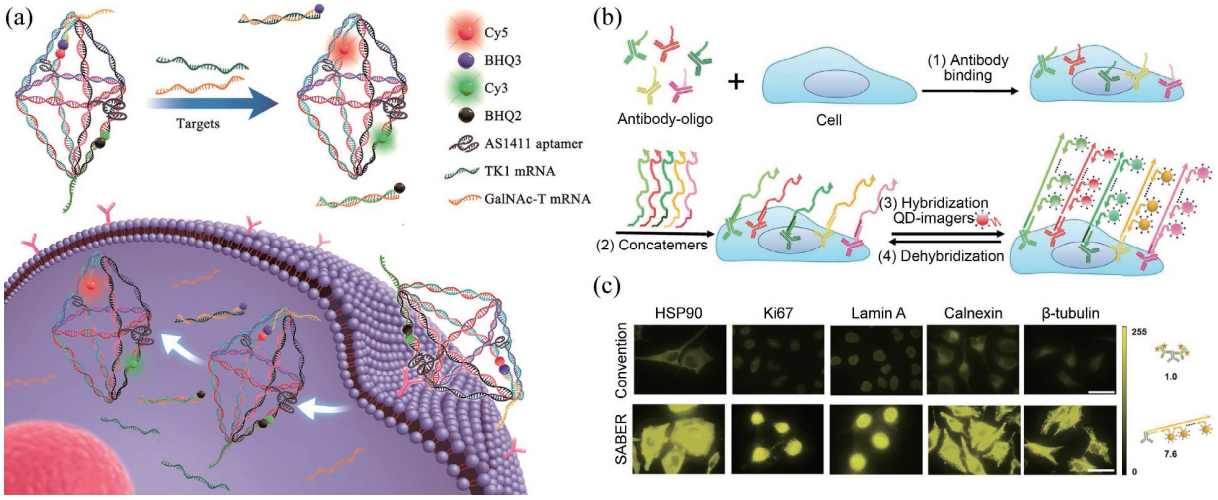

Figure 11 DNA-conjugated fluorescent entities for bioimaging. (a) Schematic diagram of the imaging of tumor-associated mRNA with fluorescent DNA probes coupled to fluorescent dyes. Reproduced with permission from Ref. [154], © American Chemical Society 2018. (b) Schematic diagram of quantum dot and signal amplification by exchange reaction (QD-SABER) for multicolor and multiplexed IHC imaging. (c) Compared with the method using conventional organic dye, the fluorescence intensity of QD-SABER in IHC imaging can be increased by 7.6 times. Reproduced with permission from Ref. [158], © Wiley-VCH Verlag GmbH & Co. KGaA, Weinheim 2020.

immunohistochemical protein imaging procedures, this method can achieve 7.6-fold signal amplification (Fig. 11(c)). Furthermore, DNA hybridization-based immunohistochemistry (IHC) can be removed to provide regenerated samples for subsequent immunostaining cycles, which in turn greatly improves their multiplexing capabilities. The combination of QDs and DNA nanomaterials is expected to improve the sensitivity and specificity of biomolecular imaging.

Zheng et al. first introduced thiol-terminated aptamer on the surface of gold nanoparticles [159]. Furthermore, a novel nanoparticle probe was prepared by hybridizing the aptamer with the short complementary Cy5 reporter strand through base complementary pairing. Initially, the fluorophore and the gold nanoparticles were close to each other, showing that the fluorescence is quenched by the gold particles. In the presence of ATP molecules, ATP binds to the aptamer with high affinity, resulting in the dissociation of the Cy5 reporter strand and realizing the turn-on of the fluorescent signal. The authors imaged the distribution of ATP in live HeLa cells by the fluorescent signal of the probe. In addition, Tan et al. also modified ferrocene-DNA on the surface of persistent luminescence nanoparticles (PLNPs) to prepare a probe that can realize electron transfer imaging *in vivo* biochemical reactions [152]. The electrons transferred during the biochemical reaction can flow to the PLNPs through the ferrocene-DNA aptamer and change their electron distribution, thereby changing the optical signal of the PLNPs. The authors successfully applied this electron transfer-triggered imaging probe to monitor the related signaling pathways. The combination of PLNPs with DNA enables precise visualization of electron transfer processes in living organisms and provides a general platform for monitoring the spatiotemporal distribution of disease-related biomolecules.

Due to the specific recognition of metal ions, DNAzyme has been used to construct sensors for metal ions. Many diseases are associated with disruption of metal homeostasis in the body. Therefore, it is essential to develop probes that can recognize specified metal ions and image their subcellular localization. To this end, a series of research has been done. For example, Wang et al. constructed the three-stranded DNAzyme precursor-gold nanoshell imaging probe (TSDP-AuNS) and the TSDP was inactivated initially [160]. When TSDP-AuNS was delivered to the interior of cell, near-infrared light is applied to release the DNAzyme from the TSDP-AuNS, restoring the activity of DNAzyme. At this time, the substrate of DNAzyme will be cleaved by the Zn^{2+}, and the fluorescence originally quenched by gold on the substrate will be recovered, realizing the imaging of Zn^{2+} in living cells (Fig. 12(a)). To further verify the imaging performance of the probes, the probes were incubated with HeLa cells for 6 h. It can be observed that the fluorescence intensity of cells was significantly increased after the addition of Zn^{2+} (Fig. 12(b)), which provides a powerful tool for intracellular metal ion imaging. To better understand the distribution and fluctuation of metal ions, a DNAzyme fluorescence sensor based on bioorthogonal reactions was developed to image Mg^{2+} in living cells [161]. An endonuclease I-SceI response site was designed on the DNAzyme. When I-SceI was expressed in cells, it cleaved the response site, switching the DNAzyme to an active conformation. The activated DNAzyme sensor then specifically catalyzed the cleavage of substrate strands in the existence of Mg^{2+}, releasing fluorescently labeled DNA fragments and generating fluorescent signals. Both confocal laser imaging and flow cytometry results demonstrated that DNAzyme-based probe had a clear response signal to Mg^{2+} compared with the negative control.

By virtue of the precise identification of miRNAs, some studies have used DNAzyme as a signal amplification tool for miRNA imaging. In 2017, Peng and collaborators designed a DNAzyme motor system to image miRNAs in living cells [162]. Specifically, multiple substrate strands and DNAzyme in a locked state were modified on the surface of gold nanoparticles. On the one hand, the location of the target miRNA can be determined by the fluorescence of the locked strand. On the other hand, the DNAzyme motor cleaved the substrate strands on the gold nanoparticles step by step, releasing the FAM-labeled DNA strands. The increase in fluorescence was proportional to the amount of target miRNA in the cell, enabling *in situ* signal amplification detection of miRNAs in living cells. Applying a similar principle, Gao et al. designed a miR-21-responsive DNAzyme walker [163]. The imaging performance of miRNAs was evaluated in tumor tissue in mice, and it was found that the fluorescence signal of DNAzyme walker was only detected at the tumor site, and the fluorescence brightness increased with time. The nanowalker accumulated and existed in tumor tissues for more than 16 h, with the potential for long-term imaging of miRNAs in living cells.

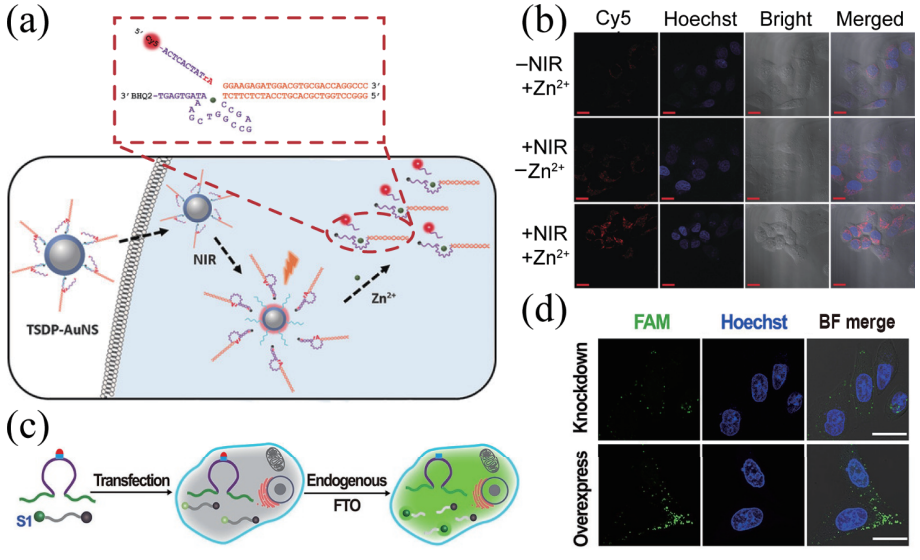

Figure 12 DNA nanomaterials with enzymatic properties for bioimaging. (a) Schematic illustration of TSDP-AuNS for intracellular Zn^{2+} imaging. (b) Confocal microscopy images of HeLa cells treated under different conditions. Reproduced with permission from Ref. [160], © Wiley-VCH Verlag GmbH & Co. KGaA, Weinheim 2017. (c) Schematic illustration of FTO-responsive DNAzyme imaging of intracellular FTO. (d) Confocal images of FTO inhibited or overexpressed in MCF7 cells. Reproduced with permission from Ref. [164], © American Chemical Society 2021.

Wang and coworkers designed a refined N6-methyladenine (m^6A) caged DNAzyme system that is specifically activated by FTO (fat mass and obesity-associated protein) [164]. Catalytically active DNAzyme was inactivated by site-specific modification of m^6A. Subsequently, DNAzyme activity was restored by FTO-mediated m^6A-cage group removal. The substrate was cleaved and the fluorescent signal was detected (Fig. 12(c)). Experiments showed that DNAzyme can reliably and accurately monitor FTO in living cells (Fig. 12(d)).

3.3 Drug delivery and therapy

As a carrier, DNA nanomaterials can provide sufficient sites and spaces for drug molecules [116, 165, 166]. In response to a specific biological environment, DNA nanomaterials could release drugs efficiently to achieve disease treatment [167–169]. In addition, DNA itself can also serve as a very potential therapeutic agent suitable for gene therapy [170]. Emerging DNA nanomaterials have been broadly explored for drug delivery and disease treatment, which we will focus on in this part.

It is critical to deliver drugs to target cells accurately and effectively. Ouyang et al. constructed a DNA nanoscale precision-guided missile (D-PGM) consisting of two parts: a warhead (WH) and a guidance/control (GC) [171]. WH was a rod-like DNA nanostructure that can efficiently load DOX, a drug which has been applied for treatment of different cancers. GC was a DNA logic circuit composed of Sgc8, Sgc4f, and TC01 aptamers. When the DOX-carrying D-PGM recognized tumor cells expressing the three target proteins simultaneously, the Sgc8, Sgc4f, and TC01 aptamers were sequentially detached from the DNA nanocarriers. The GC logic circuit is disassembled to guide DOX-loaded WH into tumor cells. D-PGM was used to precisely deliver the DOX to tumor cells, reducing the biological toxicity of DOX to normal cells and tissues caused by off-target effects. Hyperbranched polymers (HBP) can enhance drug-carrying capacity due to their unique internal cavity and three-dimensional topology. Based on this feature, Yang et al. achieved the efficient coupling of hydrophilic aptamers and hydrophobic HBP through bioorthogonal click chemistry to prepare HBP-DNA nanoparticle (HDNP) [172]. The hyperbranched side chains carried a large number of hydrophobic photo-responsive chemical groups, which can effectively load DOX with the help of internal hydrophobic interactions. The aptamer guided the nanocarrier to target the specific area. After applying ultraviolet light stimulation, the photosensitive hydrophobic group of the side chain would be rapidly degraded to form a carboxyl group, thereby enhancing the hydrophilicity of the inner core of the micelle and cleaving the micelle to achieve effective DOX release (Fig. 13(a)). The loading and release of DOX were assessed by the *in vitro* therapeutic effect, and the DOX-loaded HDNP showed significantly higher cytotoxicity, which was consistent with expectations (Fig. 13(b)). This light-responsive HDNP is an efficient drug delivery platform with great potential in cancer therapy.

Due to the controllable size and shape, good stability, and the availability of multiple binding sites, DNA origami has received extensive interest in the construction of multivalent and multifunctional drug carriers. Zhuang and colleagues constructed

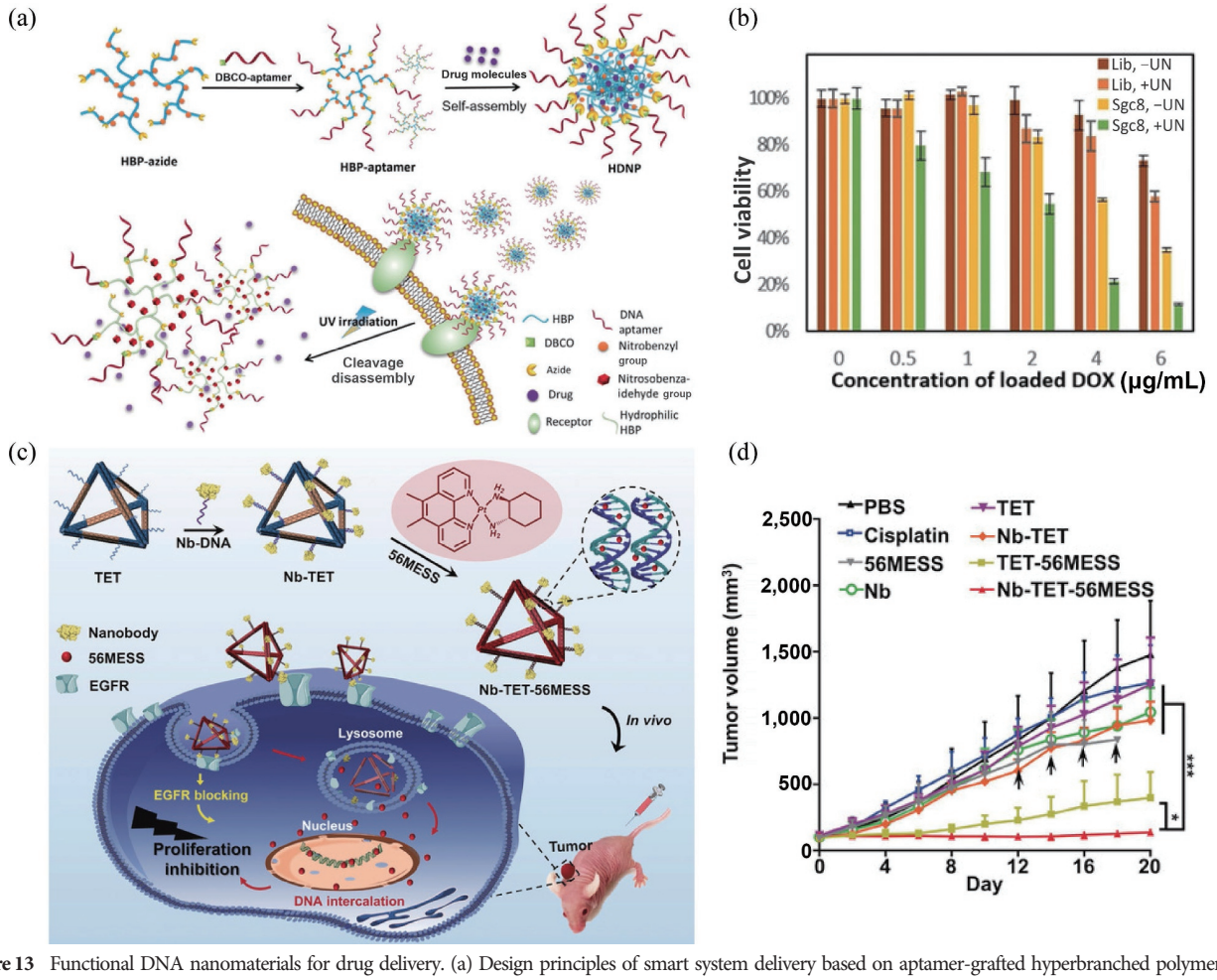

Figure 13 Functional DNA nanomaterials for drug delivery. (a) Design principles of smart system delivery based on aptamer-grafted hyperbranched polymers. (b) Cytotoxicity results from cells with different treatment. Reproduced with permission from Ref. [172], © Wiley-VCH Verlag GmbH & Co. KGaA, Weinheim 2018. (c) Schematic of nanobody-conjugated DNA nanoplatform for platinum drug delivery. (d) Tumor volume after different treatments. Reproduced with permission from Ref. [174], © Wiley-VCH Verlag GmbH & Co. KGaA, Weinheim 2019.

triangular DNA nanostructures based on DNA origami, and the negatively charged DNA double helix had a perfect binding affinity with the positively charged photosensitizer 3,6-bis[2-(1-methylpyridinium) ethynyl]-9-pentylcarbazole diiodide (BMEPC) [173]. DNA origami provided a large number of binding sites for BMEPC, which can load BMEPC in large quantities. The hydrophilicity of DNA increased the solubility of BMEPC. In addition, combined with DNA origami, the problem of low quantum yield of BMEPC was significantly improved. This may be because the free rotation of the BMEPC aromatic group is sterically restricted after binding to the DNA double helix. Under light conditions, BMEPC generated a large amount of active free radicals reactive oxygen species (ROS), which accelerated the degradation of the carrier and induced cell apoptosis.

DNA polyhedron can also serve as an ideal platform for integrating recognition units with chemotherapeutic drugs. Double-bundle DNA TET was constructed first, and the epidermal growth factor receptor-binding nanobody (Nb) was subsequently modified on TET. Wu et al. verified the successful fabrication of Nb-TET by fluorescence colocalization experiments [174]. The platinum drug 56MESS with an aromatic ring structure is inserted into the DNA double-strand by hydrophobic interaction. On the one hand, Nbs can target epidermal growth factor receptor (EGFR) on the surface of tumor cells, block EGFR signal transduction, and inhibit tumor cell proliferation. On the other hand, the release of platinum drugs can efficiently kill tumor cells (Fig. 13(c)). The anti-tumor efficacy of DNA nanocarriers was studied by tail vein injection in mice. It was found that the growth of tumors in mice was obviously inhibited, realizing targeted and combined tumor therapy (Fig. 13(d)). Similarly, Ma et al. developed a drug conjugate HApt-tFNA@DM1 using an aptamer-modified DNA tetrahedron targeting HER2 in combination with the microtubule inhibitor maytansine (DM1) [175]. Modifying DM1 at the ssDNA end of HApt-tFNA can improve the previous drug/carrier ratio of 1:1 to 3:1, increasing the drug loading efficiency. Compared with other drug formulations, this design has a better inhibitory effect on HER2-positive cancers and exhibits excellent biosafety.

In addition to delivering the above-mentioned small-molecule drugs, DNA nanomaterials are also often employed to deliver oligonucleotide drugs. A new concept of constructing DNA nanostructures by metal coordination-driven self-assembly is proposed for the first time by Li et al. [176]. Utilizing the strong coordination between DNA and metal ions, Fe-DNA nanostructures with spherical morphologies can be obtained rapidly at a high yield in water. Oligodeoxynucleotides containing unmethylated cytosine-phosphate-guanosine (CpG) have potent immunostimulatory effects and have been used as adjuvants in anticancer immunotherapy. Regarding DNA nanostructures as delivery vehicles of CpG, precise size control of nanomaterial can be achieved by adjusting the ratio of Fe^{II} ions to CpG. The results of *in vitro* and *in vivo* experiments showed that the delivery of the spherical structure as a carrier effectively increased the cellular uptake of CpG, enhancing innate immune responses by activating a variety of immune effector cells.

Besides, rolling circular amplification (RCA) can generate long ssDNA with periodic sequences for gene therapy by encapsulating abundant siRNA. Chen and coworkers synthesized DNA nanoribbons (DNRs) by combining RCA and DNA origami techniques [177]. DNRs were prepared by combining the RCA product as a scaffold with three additional short strands or one long tandem strand. Due to the unique shape and structural rigidity, DNRs can efficiently internalize into cells and escape from endosomes. The siRNA was loaded on the NDRs by thiol exchange (Fig. 14(a)). It was proved that the nanobelt loaded with siRNA could effectively downregulate the mRNA expression (Fig. 14(b)) and protein production (Fig. 14(c)) of surviving (apoptosis inhibitor), achieving efficient gene silencing and tumor therapy. This method provides an ingenious idea for siRNA delivery system based on DNA nanotechnology. As an important tumor suppressor gene, p53 has received extensive attention in gene therapy. Liu et al. realized the combination of gene therapy and chemotherapy based on DNA nanostructures [178]. Triangular DNA origami was first designed to load DOX, which was then hybridized with the tumor suppressor gene p53 to form nanokite assemblies (Fig. 14(d)). The functional DNA nanomaterial can simultaneously deliver p53 and DOX to the tumor area, and both *in vitro* and *in vivo* experimental results showed significant anti-tumor effects.

Excitingly, vesicles assembled with DNA nanostructures as biomimetic templates are also unique tools for drug delivery into cells. By precisely manipulating modular DNA nanostructures, the size and shape of vesicles can be controlled with nanoscale precision [111]. The biomimetic vesicles have good biocompatibility and are also easy to be surface-modified and encapsulated [179]. Due to their unique properties, vesicles serve as novel biomimetic drug carriers with significantly enhanced encapsulation stability for efficient delivery of therapeutic drugs.

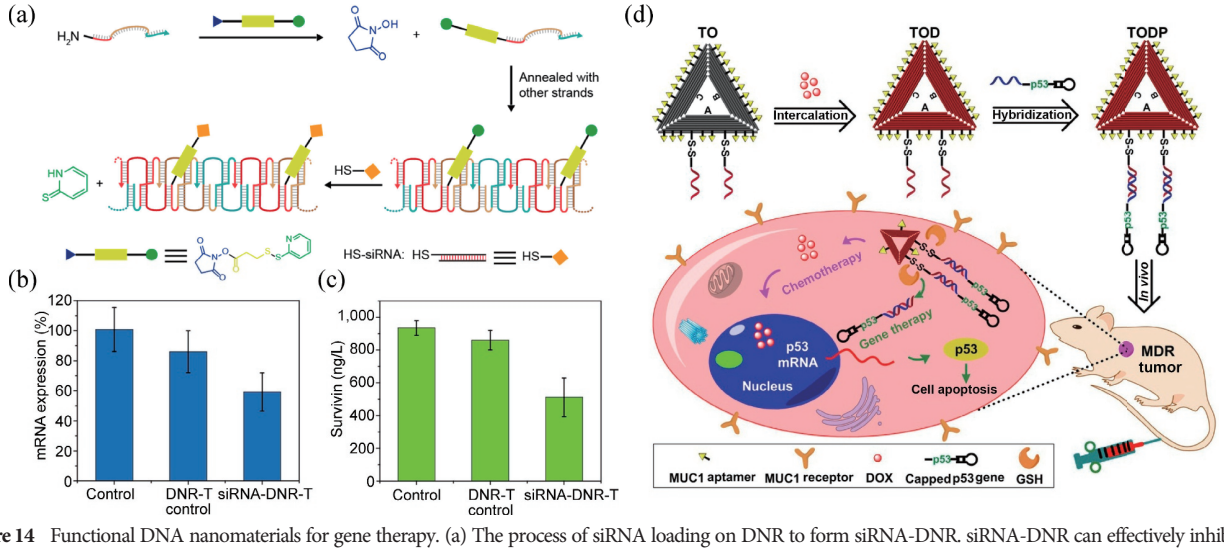

Figure 14 Functional DNA nanomaterials for gene therapy. (a) The process of siRNA loading on DNR to form siRNA-DNR. siRNA-DNR can effectively inhibit the surviving expression of (b) mRNA and (c) protein. Reproduced with permission from Ref. [177], © American Chemical Society 2015. (d) Schematic illustration of the synergy of DNA origami materials for gene therapy and chemotherapy. Reproduced with permission from Ref. [178], © American Chemical Society 2018.

Moreover, multiple therapeutic drugs can be loaded at the same time to achieve synergistic treatment of diseases, improve treatment efficiency, and reduce side effects [180]. This marks another step forward in the design of vesicles as therapeutic drug vehicles, potentially opening avenues for generating novel multifunctional drug carriers.

4 Conclusions and prospect

In the past few decades, with the rapid progress of DNA nanotechnology, DNA nanomaterials have attracted extensive attention. DNA nanomaterials with different structures have been prepared, such as DNA hydrogels, tetrahedra, nanotubes, micelles, and origami. Based on external interactions such as hydrophilic and hydrophobic interactions, chemical coupling, and other methods, it can be added various functional entities to DNA nanomaterials with different structures to prepare functional DNA nanomaterials. These characteristics play an important role in biomedical application. In this review, the preparation methods of four types of functional DNA nanomaterials were introduced. And then the biomedical applications of functional DNA nanomaterials were summarized from four aspects: biosensing, bioimaging, drug delivery, and disease treatment.

Although DNA nanotechnology has achieved many breakthroughs in the biomedical field, existing research still faces some challenges. On the one hand, DNA is only composed of four nucleotides, A, T, G, and C, which limits the structural and functional complexity of DNA nanomaterials to a certain extent. Therefore, artificial bases are needed to increase chemical diversity and versatility. However, the types of artificial bases currently used for chemical modification are limited, a variety of functional groups need to be developed to enrich the types of chemical modifications. On the other hand, when DNA is designed into nanostructures or coupled with other functional groups, biosafety and immunoreactivity require further investigation. Compared with existing drug carriers, little is known about the pharmacokinetics such as absorption, distribution, metabolism, and excretion of DNA nanomaterials, which also requires researchers to further investigate. In conclusion, it is hoped that this review will deepen the understanding of functional DNA nanomaterials and advance the development of these smart materials towards real-world applications.

Acknowledgements

This work was supported by the National Natural Science Foundation of China (Nos. 21925401, 22174038, and 21904037) and the Natural Science Foundation of Hunan Province (Nos. 2022JJ20005 and 2020JJ4173).

References

[1] Ma, W. J.; Zhan, Y. X.; Zhang, Y. X.; Mao, C. C.; Xie, X. P.; Lin, Y. F. The biological applications of DNA nanomaterials: Current challenges and future directions. *Sig. Transduct. Target. Ther.* **2021**, *6*, 351.

[2] Keller, A.; Linko, V. Challenges and perspectives of DNA nanostructures in biomedicine. *Angew. Chem., Int. Ed.* **2020**, *59*, 15818–15833.

[3] Shen, L. Y.; Wang, P. F.; Ke, Y. G. DNA nanotechnology-based biosensors and therapeutics. *Adv. Healthc. Mater.* **2021**, *10*, e2002205.

[4] Levinthal, C. The mechanism of DNA replication and genetic recombination in phage. *Proc. Natl. Acad. Sci. USA* **1956**, *42*, 394–404.

[5] Rich, A. Molecular structure of the nucleic acids. *Rev. Mod. Phys.* **1959**, *31*, 191–199.

[6] Rajwar, A.; Kharbanda, S.; Chandrasekaran, A. R.; Gupta, S.; Bhatia, D. Designer, programmable 3D DNA nanodevices to probe biological systems. *ACS Appl. Bio Mater.* **2020**, *3*, 7265–7277.

[7] Madsen, M.; Gothelf, K. V. Chemistries for DNA nanotechnology. *Chem. Rev.* **2019**, *119*, 6384–6458.

[8] Paukstelis, P. J.; Nowakowski, J.; Birktoft, J. J.; Seeman, N. C. Crystal structure of a continuous three-dimensional DNA lattice. *Chem. Biol.* **2004**, *11*, 1119–1126.

[9] Seeman, N. C.; Sleiman, H. F. DNA nanotechnology. *Nat. Rev. Mater.* **2018**, *3*, 17068.

[10] Zhang, D. Y.; Seelig, G. Dynamic DNA nanotechnology using strand-displacement reactions. *Nat. Chem.* **2011**, *3*, 103–113.

[11] Kallenbach, N. R.; Ma, R. I.; Seeman, N. C. An immobile nucleic acid junction constructed from oligonucleotides. *Nature* **1983**, *305*, 829–831.

[12] Seeman, N. C. Nucleic acid junctions and lattices. *J. Theor. Biol.* **1982**, *99*, 237–247.

[13] Hong, F.; Zhang, F.; Liu, Y.; Yan, H. DNA origami: Scaffolds for creating higher order structures. *Chem. Rev.* **2017**, *117*, 12584–12640.

[14] Aldaye, F. A.; Palmer, A. L.; Sleiman, H. F. Assembling materials with DNA as the guide. *Science* **2008**, *321*, 1795–1799.

[15] Liang, H.; Zhang, X. B.; Lv, Y. F.; Gong, L.; Wang, R. W.; Zhu, X. Y.; Yang, R. H.; Tan, W. H. Functional DNA-containing nanomaterials: Cellular applications in biosensing, imaging, and targeted therapy. *Acc. Chem. Res.* **2014**, *47*, 1891–1901.

[16] Xie, S. T.; Ai, L. L.; Cui, C.; Fu, T.; Cheng, X. D.; Qu, F. L.; Tan, W. H. Functional aptamer-embedded nanomaterials for diagnostics and therapeutics. *ACS Appl. Mater. Interfaces* **2021**, *13*, 9542–9560.

[17] Qi, H. D.; Xu, Y. W.; Hu, P.; Yao, C.; Yang, D. Y. Construction and applications of DNA-based nanomaterials in cancer therapy. *Chin. Chem. Lett.* **2022**, *33*, 1131–1140.

[18] Pinheiro, A. V.; Han, D. R.; Shih, W. M.; Yan, H. Challenges and opportunities for structural DNA nanotechnology. *Nat. Nanotechnol.* **2011**, *6*, 763–772.

[19] Kwon, P. S.; Ren, S. K.; Kwon, S. J.; Kizer, M. E.; Kuo, L. L.; Xie, M.; Zhu, D.; Zhou, F.; Zhang, F. M.; Kim, D. et al. Designer DNA architecture offers precise and multivalent spatial pattern-recognition for viral sensing and inhibition. *Nat. Chem.* **2020**, *12*, 26–35.

[20] Shaikh, S.; Younis, M.; Yuan, L. D. Functionalized DNA nanostructures for bioimaging. *Coord. Chem. Rev.* **2022**, *469*, 214648.

[21] Jones, M. R.; Seeman, N. C.; Mirkin, C. A. Programmable materials and the nature of the DNA bond. *Science* **2015**, *347*, 1260901.

[22] Hendrikse, S. I. S.; Gras, S. L.; Ellis, A. V. Opportunities and challenges in DNA-hybrid nanomaterials. *ACS Nano* **2019**, *13*, 8512–8516.

[23] Li, F.; Li, J.; Dong, B. J.; Wang, F.; Fan, C. H.; Zuo, X. L. DNA nanotechnology-empowered nanoscopic imaging of biomolecules. *Chem. Soc. Rev.* **2021**, *50*, 5650–5667.

[24] Rothemund, P. W. K. Folding DNA to create nanoscale shapes and patterns. *Nature* **2006**, *440*, 297–302.

[25] Ye, D. K.; Zuo, X. L.; Fan, C. H. DNA nanotechnology-enabled interfacial engineering for biosensor development. *Annu. Rev. Anal. Chem.* **2018**, *11*, 171–195.

[26] Hua, Y.; Ma, J. M.; Li, D. C.; Wang, R. D. DNA-based biosensors for the biochemical analysis: A review. *Biosensors* **2022**, *12*, 183.

[27] Chen, R. P.; Blackstock, D.; Sun, Q.; Chen, W. Dynamic protein assembly by programmable DNA strand displacement. *Nat. Chem.* **2018**, *10*, 474–481.

[28] Yates, L. A.; Aramayo, R. J.; Pokhrel, N.; Caldwell, C. C.; Kaplan, J. A.; Perera, R. L.; Spies, M.; Antony, E.; Zhang, X. D. A structural and dynamic model for the assembly of replication protein A on single-stranded DNA. *Nat. Commun.* **2018**, *9*, 5447.

[29] Park, S. Y.; Lytton-Jean, A. K. R.; Lee, B.; Weigand, S.; Schatz, G. C.; Mirkin, C. A. DNA-programmable nanoparticle crystallization. *Nature* **2008**, *451*, 553–556.

[30] Chou, L. Y. T.; Zagorovsky, K.; Chan, W. C. W. DNA assembly of nanoparticle superstructures for controlled biological delivery and elimination. *Nat. Nanotechnol.* **2014**, *9*, 148–155.

[31] Majewski, P. W.; Michelson, A.; Cordeiro, M. A. L.; Tian, C.; Ma, C. L.; Kisslinger, K.; Tian, Y.; Liu, W. Y.; Stach, E. A.; Yager, K. G. et al. Resilient three-dimensional ordered architectures assembled from nanoparticles by DNA. *Sci. Adv.* **2021**, *7*, eabf0617.

[32] Wang, K. L.; You, M. X.; Chen, Y.; Han, D.; Zhu, Z.; Huang, J.; Williams, K.; Yang, C. J.; Tan, W. H. Self-assembly of a bifunctional DNA carrier for drug delivery. *Angew. Chem., Int. Ed.* **2011**, *50*, 6098–6101.

[33] Hu, Q. Q.; Li, H.; Wang, L. H.; Gu, H. Z.; Fan, C. H. DNA nanotechnology-enabled drug delivery systems. *Chem. Rev.* **2019**, *119*, 6459–6506.

[34] Xu, W. T.; He, W. C.; Du, Z. H.; Zhu, L. Y.; Huang, K. L.; Lu, Y.; Luo, Y. B. Functional nucleic acid nanomaterials: Development, properties, and applications. *Angew. Chem., Int. Ed.* **2021**, *60*, 6890–6918.

[35] Li, L. L.; Xing, H.; Zhang, J. J.; Lu, Y. Functional DNA molecules enable selective and stimuli-responsive nanoparticles for biomedical applications. *Acc. Chem. Res.* **2019**, *52*, 2415–2426.

[36] Kim, J.; Jang, D.; Park, H.; Jung, S.; Kim, D. H.; Kim, W. J. Functional-DNA-driven dynamic nanoconstructs for biomolecule capture and drug delivery. *Adv. Mater.* **2018**, *30*, 1707351.

[37] Bandy, T. J.; Brewer, A.; Burns, J. R.; Marth, G.; Nguyen, T.; Stulz, E. DNA as supramolecular scaffold for functional molecules: Progress in DNA nanotechnology. *Chem. Soc. Rev.* **2011**, *40*, 138–148.

[38] Moon, W. J.; Liu, J. W. Interfacing catalytic DNA with nanomaterials. *Adv. Mater. Interfaces* **2020**, *7*, 2001017.

[39] Etzioni, R.; Urban, N.; Ramsey, S.; McIntosh, M.; Schwartz, S.; Reid, B.; Radich, J.; Anderson, G.; Hartwell, L. The case for early detection. *Nat. Rev. Cancer* **2003**, *3*, 243–252.

[40] Wang, Y.; Liu, X. L.; Wu, L. J.; Ding, L. H.; Effah, C. Y.; Wu, Y. J.; Xiong, Y. M.; He, L. L. Construction and bioapplications of aptamer-based dual recognition strategy. *Biosens. Bioelectron.* **2022**, *195*, 113661.

[41] Sefah, K.; Shangguan, D. H.; Xiong, X. L.; O'Donoghue, M. B.; Tan, W. H. Development of DNA aptamers using cell-SELEX. *Nat. Protoc.* **2010**, *5*, 1169–1185.

[42] Mayer, G.; Ahmed, M. S. L.; Dolf, A.; Endl, E.; Knolle, P. A.; Famulok, M. Fluorescence-activated cell sorting for aptamer SELEX with cell mixtures. *Nat. Protoc.* **2010**, *5*, 1993–2004.

[43] Stoltenburg, R.; Reinemann, C.; Strehlitz, B. SELEX—A (r)evolutionary method to generate high-affinity nucleic acid ligands. *Biomol. Eng.* **2007**, *24*, 381–403.

[44] Yang, G.; Zhu, C.; Zhao, L. P.; Li, L. S.; Huang, Y. Y.; Zhang, Y. K.; Qu, F. Pressure controllable aptamers picking strategy by targets competition. *Chin. Chem. Lett.* **2021**, *32*, 218–220.

[45] Ruscito, A.; DeRosa, M. C. Small-molecule binding aptamers: Selection strategies, characterization, and applications. *Front. Chem.* **2016**, *4*, 14.

[46] Hermann, T.; Patel, D. J. Adaptive recognition by nucleic acid aptamers. *Science* **2000**, *287*, 820–825.

[47] Röthlisberger, P.; Hollenstein, M. Aptamer chemistry. *Adv. Drug Deliv. Rev.* **2018**, *134*, 3–21.

[48] Dunn, M. R.; Jimenez, R. M.; Chaput, J. C. Analysis of aptamer discovery and technology. *Nat. Rev. Chem.* **2017**, *1*, 0076.

[49] Luo, J.; Isaacs, W. B.; Trent, J. M.; Duggan, D. J. Looking beyond morphology: Cancer gene expression profiling using DNA microarrays. *Cancer Invest.* **2003**, *21*, 937–949.

[50] Shangguan, D. H.; Li, Y.; Tang, Z. W.; Cao, Z. C.; Chen, H. W.; Mallikaratchy, P.; Sefah, K.; Yang, C. J.; Tan, W. H. Aptamers evolved from live cells as effective molecular probes for cancer study. *Proc. Natl. Acad. Sci. USA* **2006**, *103*, 11838–11843.

[51] Yang, X. B.; Li, N.; Gorenstein, D. G. Strategies for the discovery of therapeutic aptamers. *Expert Opin. Drug Discov.* **2011**, *6*, 75–87.

[52] Tabarzad, M.; Jafari, M. Trends in the design and development of specific aptamers against peptides and proteins. *Protein J.* **2016**, *35*, 81–99.

[53] Teng, I. T.; Li, X. W.; Yadikar, H. A.; Yang, Z. H.; Li, L.; Lyu, Y.; Pan, X. S.; Wang, K. K.; Tan, W. H. Identification and characterization of DNA aptamers specific for phosphorylation epitopes of tau protein. *J. Am. Chem. Soc.* **2018**, *140*, 14314–14323.

[54] Wang, Y. J.; Liu, M. Y.; Gao, J. L. Enhanced receptor binding of SARS-CoV-2 through networks of hydrogen-bonding and hydrophobic interactions. *Proc. Natl. Acad. Sci. USA* **2020**, *117*, 13967–13974.

[55] Song, Y. L.; Song, J.; Wei, X. Y.; Huang, M. J.; Sun, M.; Zhu, L.; Lin, B. Q.; Shen, H. C.; Zhu, Z.; Yang, C. Y. Discovery of aptamers targeting the receptor-binding domain of the SARS-CoV-2 spike glycoprotein. *Anal. Chem.* **2020**, *92*, 9895–9900.

[56] Ji, D. Y.; Lyu, K. X.; Zhao, H. Z.; Kwok, C. K. Circular L-RNA aptamer promotes target recognition and controls gene activity. *Nucleic Acids Res.* **2021**, *49*, 7280–7291.

[57] Liu, M.; Yin, Q. X.; Chang, Y. Y.; Zhang, Q.; Brennan, J. D.; Li, Y. F. *In vitro* selection of circular DNA aptamers for biosensing applications. *Angew. Chem., Int. Ed.* **2019**, *58*, 8013–8017.

[58] Mao, Y.; Gu, J.; Chang, D. R.; Wang, L.; Yao, L. L.; Ma, Q. H.; Luo, Z. F.; Qu, H.; Li, Y. F.; Zheng, L. Evolution of a highly functional circular DNA aptamer in serum. *Nucleic Acids Res.* **2020**, *48*, 10680–10690.

[59] Yoshikawa, A. M.; Rangel, A.; Feagin, T.; Chun, E. M.; Wan, L.; Li, A. P.; Moeckl, L.; Wu, D. N.; Eisenstein, M.; Pitteri, S. et al. Discovery of indole-modified aptamers for highly specific recognition of protein glycoforms. *Nat. Commun.* **2021**, *12*, 7106.

[60] Cheung, Y. W.; Röthlisberger, P.; Mechaly, A. E.; Weber, P.; Levi-Acobas, F.; Lo, Y.; Wong, A. W. C.; Kinghorn, A. B.; Haouz, A.; Savage, G. P. et al. Evolution of abiotic cubane chemistries in a nucleic acid aptamer allows selective recognition of a malaria biomarker. *Proc. Natl. Acad. Sci. USA* **2020**, *117*, 16790–16798.

[61] Tan, J.; Zhao, M. M.; Wang, J.; Li, Z. H.; Liang, L.; Zhang, L. Q.; Yuan, Q.; Tan, W. H. Regulation of protein activity and cellular functions mediated by molecularly evolved nucleic acids. *Angew. Chem., Int. Ed.* **2019**, *58*, 1621–1625.

[62] Jiang, D. W.; Ni, D. L.; Rosenkrans, Z. T.; Huang, P.; Yan, X. Y.; Cai, W. B. Nanozyme: New horizons for responsive biomedical applications. *Chem. Soc. Rev.* **2019**, *48*, 3683–3704.

[63] Lin, Y. H.; Ren, J. S.; Qu, X. G. Nano-gold as artificial enzymes: Hidden talents. *Adv. Mater.* **2014**, *26*, 4200–4217.

[64] Yu, Z. Z.; Lou, R. X.; Pan, W.; Li, N.; Tang, B. Nanoenzymes in disease diagnosis and therapy. *Chem. Commun.* **2020**, *56*, 15513–15524.

[65] Wang, H.; Wan, K. W.; Shi, X. H. Recent advances in nanozyme research. *Adv. Mater.* **2019**, *31*, e1805368.

[66] Chen, M.; Zhou, H.; Liu, X. K.; Yuan, T. W.; Wang, W. Y.; Zhao, C.; Zhao, Y. F.; Zhou, F. Y.; Wang, X.; Xue, Z. et al. Single iron site nanozyme for ultrasensitive glucose detection. *Small* **2020**, *16*, 2002343.

[67] Li, S. S.; Shang, L.; Xu, B. L.; Wang, S. H.; Gu, K.; Wu, Q. Y.; Sun, Y.; Zhang, Q. H.; Yang, H. L.; Zhang, F. R. et al. A nanozyme with photo-enhanced dual enzyme-like activities for deep pancreatic cancer therapy. *Angew. Chem., Int. Ed.* **2019**, *58*, 12624–12631.

[68] Breaker, R. R.; Joyce, G. F. A DNA enzyme that cleaves RNA. *Chem. Biol.* **1994**, *1*, 223–229.

[69] Rostovtsev, V. V.; Green, L. G.; Fokin, V. V.; Sharpless, K. B. A stepwise huisgen cycloaddition process: Copper(I)-catalyzed regioselective "ligation" of azides and terminal alkynes. *Angew. Chem., Int. Ed.* **2002**, *41*, 2596–2599.

[70] Liu, K.; Lat, P. K.; Yu, H. Z.; Sen, D. Click-17, a DNA enzyme that harnesses ultra-low concentrations of either Cu^{+} or Cu^{2+} to catalyze the azide-alkyne "click" reaction in water. *Nucleic Acids Res.* **2020**, *48*, 7356–7370.

[71] Ali, M. M.; Wolfe, M.; Tram, K.; Gu, J.; Filipe, C. D. M.; Li, Y. F.; Brennan, J. D. A DNAzyme-based colorimetric paper sensor for *Helicobacter pylori*. *Angew. Chem., Int. Ed.* **2019**, *58*, 9907–9911.

[72] Wang, Y. J.; Nguyen, K.; Spitale, R. C.; Chaput, J. C. A biologically stable DNAzyme that efficiently silences gene expression in cells. *Nat. Chem.* **2021**, *13*, 319–326.

[73] Wei, Z. H.; Yu, Y. F.; Hu, S. Q.; Yi, X. Y.; Wang, J. X. Bifunctional diblock DNA-mediated synthesis of nanoflower-shaped photothermal nanozymes for a highly sensitive colorimetric assay of cancer cells. *ACS Appl. Mater. Interfaces* **2021**, *13*, 16801–16811.
[74] Li, K.; Wang, K.; Qin, W. W.; Deng, S. H.; Li, D.; Shi, J. Y.; Huang, Q.; Fan, C. H. DNA-directed assembly of gold nanohalo for quantitative plasmonic imaging of single-particle catalysis. J. Am. *Chem. Soc.* **2015**, *137*, 4292–4295.
[75] Satyavolu, N. S. R.; Tan, L. H.; Lu, Y. DNA-mediated morphological control of Pd-Au bimetallic nanoparticles. J. Am. *Chem. Soc.* **2016**, *138*, 16542–16548.
[76] Lu, C.; Tang, L. H.; Gao, F.; Li, Y. Z.; Liu, J. W.; Zheng, J. K. DNA-encoded bimetallic Au-Pt dumbbell nanozyme for high-performance detection and eradication of *Escherichia coli O157: H7*. *Biosens. Bioelectron* **2021**, *187*, 113327.
[77] Zhang, Y.; Chan, H. F.; Leong, K. W. Advanced materials and processing for drug delivery: The past and the future. *Adv. Drug Deliv. Rev.* **2013**, *65*, 104–120.
[78] Khezri, B.; Beladi Mousavi, S. M.; Krejčová, L.; Heger, Z.; Sofer, Z.; Pumera, M. Ultrafast electrochemical trigger drug delivery mechanism for nanographene micromachines. *Adv. Funct. Mater.* **2019**, *29*, 1806696.
[79] Shen, S. H.; Wu, Y. S.; Liu, Y. C.; Wu, D. C. High drug-loading nanomedicines: Progress, current status, and prospects. *Int. J. Nanomed.* **2017**, *12*, 4085–4109.
[80] Han, S. Y.; Samanta, A.; Xie, X. J.; Huang, L.; Peng, J. J.; Park, S. J.; Teh, D. B. L.; Choi, Y.; Chang, Y. T.; All, A. H. et al. Gold and hairpin DNA functionalization of upconversion nanocrystals for imaging and *in vivo* drug delivery. *Adv. Mater.* **2017**, *29*, 1700244.
[81] Li, J.; Fan, C. H.; Pei, H.; Shi, J. Y.; Huang, Q. Smart drug delivery nanocarriers with self-assembled DNA nanostructures. *Adv. Mater.* **2013**, *25*, 4386–4396.
[82] Zhang, H. M.; Ma, Y. L.; Xie, Y.; An, Y.; Huang, Y. S.; Zhu, Z.; Yang, C. J. A controllable aptamer-based self-assembled DNA dendrimer for high affinity targeting, bioimaging and drug delivery. *Sci. Rep.* **2015**, *5*, 10099.
[83] Roberts, T. C.; Langer, R.; Wood, M. J. A. Advances in oligonucleotide drug delivery. *Nat. Rev. Drug Discov.* **2020**, *19*, 673–694.
[84] Venkataraman, S.; Hedrick, J. L.; Ong, Z. Y.; Yang, C.; Ee, P. L. R.; Hammond, P. T.; Yang, Y. Y. The effects of polymeric nanostructure shape on drug delivery. *Adv. Drug Deliv. Rev.* **2011**, *63*, 1228–1246.
[85] Shao, Y.; Jia, H. Y.; Cao, T. Y.; Liu, D. S. Supramolecular hydrogels based on DNA self-assembly. *Acc. Chem. Res.* **2017**, *50*, 659–668.
[86] Huang, F. J.; Chen, M. X.; Zhou, Z. X.; Duan, R. L.; Xia, F.; Willner, I. Spatiotemporal patterning of photoresponsive DNA-based hydrogels to tune local cell responses. *Nat. Commun.* **2021**, *12*, 2364.
[87] Zhang, J.; Guo, Y. Y.; Pan, G. F.; Wang, P.; Li, Y. H.; Zhu, X. Y.; Zhang, C. Injectable drug-conjugated DNA hydrogel for local chemotherapy to prevent tumor recurrence. *ACS Appl. Mater. Interfaces* **2020**, *12*, 21441–21449.
[88] Hu, Y. W.; Gao, S. J.; Lu, H. F.; Ying, J. Y. Acid-resistant and physiological pH-responsive DNA hydrogel composed of A-motif and i-motif toward oral insulin delivery. *J. Am. Chem. Soc.* **2022**, *144*, 5461–5470.
[89] Ding, F.; Mou, Q. B.; Ma, Y.; Pan, G. F.; Guo, Y. Y.; Tong, G. S.; Choi, C. H. J.; Zhu, X. Y.; Zhang, C. A crosslinked nucleic acid nanogel for effective siRNA delivery and antitumor therapy. *Angew. Chem., Int. Ed.* **2018**, *57*, 3064–3068.
[90] Zhang, J.; Guo, Y. Y.; Ding, F.; Pan, G. F.; Zhu, X. Y.; Zhang, C. A camptothecin-grafted DNA tetrahedron as a precise nanomedicine to inhibit tumor growth. *Angew. Chem., Int. Ed.* **2019**, *58*, 13794–13798.
[91] Xiao, D. X.; Li, Y. J.; Tian, T. R.; Zhang, T. X.; Shi, S. R.; Lu, B. Y.; Gao, Y.; Qin, X.; Zhang, M.; Wei, W. et al. Tetrahedral framework nucleic acids loaded with aptamer AS1411 for siRNA delivery and gene silencing in malignant melanoma. *ACS Appl. Mater. Interfaces* **2021**, *13*, 6109–6118.
[92] Fu, W.; Ma, L.; Ju, Y.; Xu, J. G.; Li, H.; Shi, S. R.; Zhang, T.; Zhou, R. H.; Zhu, J. W.; Xu, R. et al. Therapeutic siCCR2 loaded by tetrahedral framework DNA nanorobotics in therapy for intracranial hemorrhage. *Adv. Funct. Mater.* **2021**, *31*, 2101435.
[93] Wang, D.; Peng, R. Z.; Peng, Y. B.; Deng, Z. Y.; Xu, F. Y.; Su, Y. Y.; Wang, P. E.; Li, L.; Wang, X. Q.; Ke, Y. G. et al. Hierarchical fabrication of DNA wireframe nanoarchitectures for efficient cancer imaging and targeted therapy. *ACS Nano* **2020**, *14*, 17365–17375.
[94] Wang, Z. R.; Song, L. L.; Liu, Q.; Tian, R.; Shang, Y. X.; Liu, F. S.; Liu, S. L.; Zhao, S.; Han, Z. H.; Sun, J. S. et al. A tubular DNA nanodevice as a siRNA/chemo-drug co-delivery vehicle for combined cancer therapy. *Angew. Chem., Int. Ed.* **2021**, *60*, 2594–2598.
[95] Zhang, L. L.; Abdullah, R.; Hu, X. X.; Bai, H. R.; Fan, H. H.; He, L.; Liang, H.; Zou, J. M.; Liu, Y. L.; Sun, Y. et al. Engineering of bioinspired, size-controllable, self-degradable cancer-targeting DNA nanoflowers via the incorporation of an artificial sandwich base. *J. Am. Chem. Soc.* **2019**, *141*, 4282–4290.
[96] Willem de Vries, J.; Schnichels, S.; Hurst, J.; Strudel, L.; Gruszka, A.; Kwak, M.; Bartz-Schmidt, K. U.; Spitzer, M. S.; Herrmann, A. DNA nanoparticles for ophthalmic drug delivery. *Biomaterials* **2018**, *157*, 98–106.
[97] Shang, Y. X.; Li, N.; Liu, S. B.; Wang, L.; Wang, Z. G.; Zhang, Z.; Ding, B. Q. Site-specific synthesis of silica nanostructures on DNA origami templates. *Adv. Mater.* **2020**, *32*, 2000294.
[98] Dey, S.; Fan, C. H.; Gothelf, K. V.; Li, J.; Lin, C. X.; Liu, L. F.; Liu, N.; Nijenhuis, M. A. D.; Saccà, B.; Simmel, F. C. et al. DNA origami. *Nat. Rev. Methods Primers* **2021**, *1*, 13.
[99] Tokura, Y.; Jiang, Y. Y.; Welle, A.; Stenzel, M. H.; Krzemien, K. M.; Michaelis, J.; Berger, R.; Barner-Kowollik, C.; Wu, Y. Z.; Weil, T. Bottom-up fabrication of nanopatterned polymers on DNA origami by *in situ* atom-transfer radical polymerization. *Angew. Chem., Int. Ed.* **2016**, *55*, 5692–5697.
[100] Fan, S. S.; Wang, D. F.; Kenaan, A.; Cheng, J.; Cui, D. X.; Song, J. Create nanoscale patterns with DNA origami. *Small* **2019**, *15*, 1805554.
[101] Li, N.; Shang, Y. X.; Xu, R.; Jiang, Q.; Liu, J. B.; Wang, L.; Cheng, Z. H.; Ding, B. Q. Precise organization of metal and metal oxide nanoclusters into arbitrary patterns on DNA origami. *J. Am. Chem. Soc.* **2019**, *141*, 17968–17972.
[102] Jun, H.; Zhang, F.; Shepherd, T.; Ratanalert, S.; Qi, X. D.; Yan, H.; Bathe, M. Autonomously designed free-form 2D DNA origami. *Sci. Adv.* **2019**, *5*, eaav0655.
[103] Edwardson, T. G. W.; Lau, K. L.; Bousmail, D.; Serpell, C. J.; Sleiman, H. F. Transfer of molecular recognition information from DNA nanostructures to gold nanoparticles. *Nat. Chem.* **2016**, *8*, 162–170.
[104] Shi, P.; Zhao, N.; Coyne, J.; Wang, Y. DNA-templated synthesis of biomimetic cell wall for nanoencapsulation and protection of mammalian cells. *Nat. Commun.* **2019**, *10*, 2223.
[105] Storhoff, J. J.; Mirkin, C. A. Programmed materials synthesis with DNA. *Chem. Rev.* **1999**, *99*, 1849–1862.
[106] Zhao, H. W.; Liu, S. J.; Wei, Y.; Yue, Y. H.; Gao, M. R.; Li, Y. B.; Zeng, X. L.; Deng, X. L.; Kotov, N. A.; Guo, L. et al. Multiscale engineered artificial tooth enamel. *Science,* **2022**, *375*, 551–556.
[107] Zhou, Y. S.; Deng, J. J.; Zhang, Y.; Li, C.; Wei, Z.; Shen, J. L.; Li, J. J.; Wang, F.; Han, B.; Chen, D. et al. Engineering DNA-guided hydroxyapatite bulk materials with high stiffness and outstanding antimicrobial ability for dental inlay applications. *Adv. Mater.* **2022**, *34*, 2202180.
[108] Wu, S. S.; Zhang, M. Z.; Song, J.; Weber, S.; Liu, X. G.; Fan, C. H.; Wu, Y. Z. Fine customization of calcium phosphate nanostructures with site-specific modification by DNA templated mineralization. *ACS Nano* **2021**, *15*, 1555–1565.
[109] Tokura, Y.; Harvey, S.; Chen, C. J.; Wu, Y. Z.; Ng, D. Y. W.; Weil, T. Fabrication of defined polydopamine nanostructures by DNA origami-templated polymerization. *Angew. Chem., Int. Ed.* **2018**,

130, 1603–1607.
[110] Winterwerber, P.; Harvey, S.; Ng, D. Y. W.; Weil, T. Photocontrolled dopamine polymerization on DNA origami with nanometer resolution. *Angew. Chem., Int. Ed.* **2020**, *59*, 6144–6149.
[111] Yang, Y.; Wang, J.; Shigematsu, H.; Xu, W. M.; Shih, W. M.; Rothman, J. E.; Lin, C. X. Self-assembly of size-controlled liposomes on DNA nanotemplates. *Nat. Chem.* **2016**, *8*, 476–483.
[112] Zhang, Z.; Yang, Y.; Pincet, F.; Llaguno, M. C.; Lin, C. X. Placing and shaping liposomes with reconfigurable DNA nanocages. *Nat. Chem.* **2017**, *9*, 653–659.
[113] Perrault, S. D.; Shih, W. M. Virus-inspired membrane encapsulation of DNA nanostructures to achieve *in vivo* stability. *ACS Nano* **2014**, *8*, 5132–5140.
[114] Kurokawa, C.; Fujiwara, K.; Morita, M.; Kawamata, I.; Kawagishi, Y.; Sakai, A.; Murayama, Y.; Nomura, S. I. M.; Murata, S.; Takinoue, M. et al. DNA cytoskeleton for stabilizing artificial cells. *Proc. Natl. Acad. Sci. USA* **2017**, *114*, 7228–7233.
[115] Nummelin, S.; Kommeri, J.; Kostiainen, M. A.; Linko, V. Evolution of structural DNA nanotechnology. *Adv. Mater.* **2018**, *30*, 1703721.
[116] Jiang, D. W.; England, C. G.; Cai, W. B. DNA nanomaterials for preclinical imaging and drug delivery. *J. Control. Release* **2016**, *239*, 27–38.
[117] Meng, H. M.; Liu, H.; Kuai, H. L.; Peng, R. Z.; Mo, L. T.; Zhang, X. B. Aptamer-integrated DNA nanostructures for biosensing, bioimaging and cancer therapy. *Chem. Soc. Rev.* **2016**, *45*, 2583–2602.
[118] Zhang, J. J.; Lan, T.; Lu, Y. Molecular engineering of functional nucleic acid nanomaterials toward *in vivo* applications. *Adv. Healthcare Mater.* **2019**, *8*, 1801158.
[119] Zhang, Y. Z.; Tu, J.; Wang, D. Q.; Zhu, H. T.; Maity, S. K.; Qu, X. M.; Bogaert, B.; Pei, H.; Zhang, H. B. Programmable and multifunctional DNA-based materials for biomedical applications. *Adv. Mater.* **2018**, *30*, 1703658.
[120] Du, Y.; Dong, S. J. Nucleic acid biosensors: Recent advances and perspectives. *Anal. Chem.* **2017**, *89*, 189–215.
[121] Xiao, M. S.; Lai, W.; Man, T. T.; Chang, B. B.; Li, L.; Chandrasekaran, A. R.; Pei, H. Rationally engineered nucleic acid architectures for biosensing applications. *Chem. Rev.* **2019**, *119*, 11631–11717.
[122] Yang, F.; Li, Q.; Wang, L. H.; Zhang, G. J.; Fan, C. H. Framework-nucleic-acid-enabled biosensor development. *ACS Sens.* **2018**, *3*, 903–919.
[123] Li, H. K.; Ye, H. L.; Zhao, X. X.; Sun, X. L.; Zhu, Q. Q.; Han, Z. Y.; Yuan, R. R.; He, H. M. Artful union of a zirconium-porphyrin MOF/GO composite for fabricating an aptamer-based electrochemical sensor with superb detecting performance. *Chin. Chem. Lett.* **2021**, *32*, 2851–2855.
[124] Song, P.; Li, M.; Shen, J. W.; Pei, H.; Chao, J.; Su, S.; Aldalbahi, A.; Wang, L. H.; Shi, J. Y.; Song, S. P. et al. Dynamic modulation of DNA hybridization using allosteric DNA tetrahedral nanostructures. *Anal. Chem.* **2016**, *88*, 8043–8049.
[125] Chang, D. R.; Zakaria, S.; Esmaeili Samani, S.; Chang, Y. Y.; Filipe, C. D. M.; Soleymani, L.; Brennan, J. D.; Liu, M.; Li, Y. F. Functional nucleic acids for pathogenic bacteria detection. *Acc. Chem. Res.* **2021**, *54*, 3540–3549.
[126] Zhu, X. Y.; Wang, R. Y.; Zhou, X. H.; Shi, H. C. Free-energy-driven lock/open assembly-based optical DNA sensor for cancer-related microRNA detection with a shortened time-to-result. *ACS Appl. Mater. Interfaces* **2017**, *9*, 25789–25795.
[127] Xiao, M. S.; Wang, X. W.; Li, L.; Pei, H. Stochastic RNA walkers for intracellular MicroRNA imaging. *Anal. Chem.* **2019**, *91*, 11253–11258.
[128] Xiao, M. S.; Zou, K.; Li, L.; Wang, L. H.; Tian, Y.; Fan, C. H.; Pei, H. Stochastic DNA walkers in droplets for super-multiplexed bacterial phenotype detection. *Angew. Chem., Int. Ed.* **2019**, *58*, 15448–15454.
[129] Ebrahimi, S. B.; Samanta, D.; Mirkin, C. A. DNA-based nanostructures for live-cell analysis. J. Am. *Chem. Soc.* **2020**, *142*, 11343–11356.
[130] Chai, H.; Miao, P. Ultrasensitive assay of ctDNA based on DNA triangular prism and three-way junction nanostructures. *Chin. Chem. Lett.* **2021**, *32*, 783–786.
[131] Zhang, J.; Hou, M. F.; Chen, G. Y.; Mao, H. F.; Chen, W. Q.; Wang, W. S.; Chen, J. H. An electrochemical biosensor based on DNA "nano-bridge" for amplified detection of exosomal microRNAs. *Chin. Chem. Lett.* **2021**, *32*, 3474–3478.
[132] Liu, J. M.; Zhang, Y.; Xie, H. B.; Zhao, L.; Zheng, L.; Ye, H. M. Applications of catalytic hairpin assembly reaction in biosensing. *Small* **2019**, *15*, 1902989.
[133] Wang, J.; Ma, Q. Q.; Zheng, W.; Liu, H. Y.; Yin, C. Q.; Wang, F. B.; Chen, X. Y.; Yuan, Q.; Tan, W. H. One-dimensional luminous nanorods featuring tunable persistent luminescence for autofluorescence-free biosensing. *ACS Nano* **2017**, *11*, 8185–8191.
[134] Zhan, S. S.; Wu, Y. G.; Wang, L. M.; Zhan, X. J.; Zhou, P. A mini-review on functional nucleic acids-based heavy metal ion detection. *Biosens. Bioelectron.* **2016**, *86*, 353–368.
[135] Duan, Z. J.; Tan, L. X.; Duan, R. L.; Chen, M. X.; Xia, F.; Huang, F. J. Photoactivated biosensing process for dictated ATP detection in single living cells. *Anal. Chem.* **2021**, *93*, 11547–11556.
[136] Zhu, D.; Wei, Y. Q.; Sun, T.; Zhang, C. W.; Ang, L.; Su, S.; Mao, X. H.; Li, Q.; Fan, C. H.; Zuo, X. L. et al. Encoding DNA frameworks for amplified multiplexed imaging of intracellular microRNAs. *Anal. Chem.* **2021**, *93*, 2226–2234.
[137] Wang, X. J.; Kong, D. R.; Guo, M. Q.; Wang, L. Q.; Gu, C. J.; Dai, C. H.; Wang, Y.; Jiang, Q. F.; Ai, Z. L.; Zhang, C. et al. Rapid SARS-CoV-2 nucleic acid testing and pooled assay by tetrahedral DNA nanostructure transistor. *Nano Lett.* **2021**, *21*, 9450–9457.
[138] Wu, Y. G.; Ji, D. Z.; Dai, C. H.; Kong, D. R.; Chen, Y. H.; Wang, L. Q.; Guo, M. Q.; Liu, Y. Q.; Wei, D. C. Triple-probe DNA framework-based transistor for SARS-CoV-2 10-in-1 pooled testing. *Nano Lett.* **2022**, *22*, 3307–3316.
[139] Shyu, A. B.; Wilkinson, M. F.; van Hoof, A. Messenger RNA regulation: To translate or to degrade. *EMBO J.* **2008**, *27*, 471–481.
[140] He, L.; Lu, D. Q.; Liang, H.; Xie, S. T.; Luo, C.; Hu, M. M.; Xu, L. J.; Zhang, X. B.; Tan, W. H. Fluorescence resonance energy transfer-based DNA tetrahedron nanotweezer for highly reliable detection of tumor-related mRNA in living cells. *ACS Nano* **2017**, *11*, 4060–4066.
[141] Bushati, N.; Cohen, S. M. microRNA functions. Annu. Rev. *Cell. Dev. Biol.* **2007**, *23*, 175–205.
[142] Lu, T. X.; Rothenberg, M. E. MicroRNA. *J. Allergy Clin. Immunol.* **2018**, *141*, 1202–1207.
[143] Zhu, D.; Huang, J. X.; Lu, B.; Zhu, Y.; Wei, Y. Q.; Zhang, Q.; Guo, X. X.; Yuwen, L. H.; Su, S.; Chao, J. et al. Intracellular microRNA imaging with MoS_2-supported nonenzymatic catassembly of DNA hairpins. *ACS Appl. Mater. Interfaces* **2019**, *11*, 20725–20733.
[144] Zhou, W. J.; Li, D. X.; Xiong, C. Y.; Yuan, R.; Xiang, Y. Multicolor-encoded reconfigurable DNA nanostructures enable multiplexed sensing of intracellular microRNAs in living cells. *ACS Appl. Mater. Interfaces* **2016**, *8*, 13303–13308.
[145] Chen, B.; Wang, Y. T.; Ma, W. J.; Cheng, H.; Sun, H. H.; Wang, H. Z.; Huang, J.; He, X. X.; Wang, K. M. A mimosa-inspired cell-surface-anchored ratiometric DNA nanosensor for high-resolution and sensitive response of target tumor extracellular pH. *Anal. Chem.* **2020**, *92*, 15104–15111.
[146] Zhao, J.; Gao, J. H.; Xue, W. T.; Di, Z. H.; Xing, H.; Lu, Y.; Li, L. L. Upconversion luminescence-activated DNA nanodevice for ATP sensing in living cells. *J. Am. Chem. Soc.* **2018**, *140*, 578–581.
[147] Shao, Y. L.; Zhao, J.; Yuan, J. Y.; Zhao, Y. L.; Li, L. L. Organelle-specific photoactivation of DNA nanosensors for precise profiling of subcellular enzymatic activity. *Angew. Chem., Int. Ed.* **2021**, *60*, 8923–8931.
[148] Jani, M. S.; Zou, J. Y.; Veetil, A. T.; Krishnan, Y. A DNA-based fluorescent probe maps NOS3 activity with subcellular spatial resolution. *Nat. Chem. Biol.* **2020**, *16*, 660–666.
[149] Ahmed, R.; Oborski, M. J.; Hwang, M.; Lieberman, F. S.; Mountz, J. M. Malignant gliomas: Current perspectives in diagnosis, treatment, and early response assessment using advanced quantitative imaging methods. *Cancer Manag. Res.* **2014**, *6*, 149–170.

[150] Pei, H.; Zuo, X. L.; Zhu, D.; Huang, Q.; Fan, C. H. Functional DNA nanostructures for theranostic applications. *Acc. Chem. Res.* **2014**, *47*, 550–559.
[151] Yang, Q.; Chang, X.; Lee, J. Y.; Olivera, T. R.; Saji, M.; Wisniewski, H.; Kim, S.; Zhang, F. Recent advances in self-assembled DNA nanostructures for bioimaging. *ACS Appl. Bio Mater.*, in press, https://doi.org/10.1021/acsabm.2c00128.
[152] Tan, J.; Li, H.; Ji, C. L.; Zhang, L.; Zhao, C. X.; Tang, L. M.; Zhang, C. X.; Sun, Z. J.; Tan, W. H.; Yuan, Q. Electron transfer-triggered imaging of EGFR signaling activity. *Nat. Commun.* **2022**, *13*, 594.
[153] Li, L. L.; Wu, P. W.; Hwang, K.; Lu, Y. An exceptionally simple strategy for DNA-functionalized up-conversion nanoparticles as biocompatible agents for nanoassembly, DNA delivery, and imaging. *J. Am. Chem. Soc.* **2013**, *135*, 2411–2414.
[154] Zhong, L.; Cai, S. X.; Huang, Y. Q.; Yin, L. T.; Yang, Y. L.; Lu, C. H.; Yang, H. H. DNA octahedron-based fluorescence nanoprobe for dual tumor-related mRNAs detection and imaging. *Anal. Chem.* **2018**, *90*, 12059–12066.
[155] Xiao, F.; Lin, L.; Chao, Z. C.; Shao, C.; Chen, Z.; Wei, Z. X.; Lu, J. X.; Huang, Y. S.; Li, L. Q.; Liu, Q. et al. Organic spherical nucleic acids for the transport of a NIR-II-emitting dye across the blood-brain barrier. *Angew. Chem., Int. Ed.* **2020**, *59*, 9702–9710.
[156] Tao, X. Q.; Liao, Z. Y.; Zhang, Y. Q.; Fu, F.; Hao, M. Q.; Song, Y.; Song, E. Q. Aptamer-quantum dots and teicoplanin-gold nanoparticles constructed FRET sensor for sensitive detection of *Staphylococcus aureus*. *Chin. Chem. Lett.* **2021**, *32*, 791–795.
[157] Ma, Y. X.; Mao, G. B.; Huang, W. R.; Wu, G. Q.; Yin, W.; Ji, X. H.; Deng, Z. S.; Cai, Z. M.; Zhang, X. E.; He, Z. K. et al. Quantum dot nanobeacons for single RNA labeling and imaging. *J. Am. Chem. Soc.* **2019**, *141*, 13454–13458.
[158] Zhou, W.; Han, Y.; Beliveau, B. J.; Gao, X. H. Combining Qdot nanotechnology and DNA nanotechnology for sensitive single-cell imaging. *Adv. Mater.* **2020**, *32*, 1908410.
[159] Zheng, D.; Seferos, D. S.; Giljohann, D. A.; Patel, P. C.; Mirkin, C. A. Aptamer nano-flares for molecular detection in living cells. *Nano Lett.* **2009**, *9*, 3258–3261.
[160] Wang, W. J.; Satyavolu, N. S. R.; Wu, Z. K.; Zhang, J. R.; Zhu, J. J.; Lu, Y. Near-infrared photothermally activated DNAzyme-gold nanoshells for imaging metal ions in living cells. *Angew. Chem., Int. Ed.* **2017**, *56*, 6798–6802.
[161] Lin, Y.; Yang, Z. L.; Lake, R. J.; Zheng, C. B.; Lu, Y. Enzyme-mediated endogenous and bioorthogonal control of a DNAzyme fluorescent sensor for imaging metal ions in living cells. *Angew. Chem., Int. Ed.* **2019**, *58*, 17061–17067.
[162] Peng, H. Y.; Li, X. F.; Zhang, H. Q.; Le, X. C. A microRNA-initiated DNAzyme motor operating in living cells. *Nat. Commun.* **2017**, *8*, 14378.
[163] Gao, Y. S.; Zhang, S. B.; Wu, C. W.; Li, Q.; Shen, Z. F.; Lu, Y.; Wu, Z. S. Self-protected DNAzyme walker with a circular bulging DNA shield for amplified imaging of miRNAs in living cells and mice. *ACS Nano* **2021**, *15*, 19211–19224.
[164] Wang, Q.; Tan, K. Y.; Wang, H.; Shang, J. H.; Wan, Y. Q.; Liu, X. Q.; Weng, X. C.; Wang, F. A. Orthogonal demethylase-activated deoxyribozyme for intracellular imaging and gene regulation. *J. Am. Chem. Soc.* **2021**, *143*, 6895–6904.
[165] Angell, C.; Xie, S. B.; Zhang, L. F.; Chen, Y. DNA nanotechnology for precise control over drug delivery and gene therapy. *Small* **2016**, *12*, 1117–1132.
[166] Li, J. Y.; Mooney, D. J. Designing hydrogels for controlled drug delivery. *Nat. Rev. Mater.* **2016**, *1*, 16071.
[167] Cheng, R.; Meng, F. H.; Deng, C.; Klok, H. A.; Zhong, Z. Y. Dual and multi-stimuli responsive polymeric nanoparticles for programmed site-specific drug delivery. *Biomaterials* **2013**, *34*, 3647–3657.
[168] Dai, Z. W.; Leung, H. M.; Lo, P. K. Stimuli-responsive self-assembled DNA nanomaterials for biomedical applications. *Small* **2017**, *13*, 1602881.
[169] Lu, C. H.; Willner, B.; Willner, I. DNA nanotechnology: From sensing and DNA machines to drug-delivery systems. *ACS Nano* **2013**, *7*, 8320–8332.
[170] Yuan, Y.; Gu, Z.; Yao, C.; Luo, D.; Yang, D. Y. Nucleic acid-based functional nanomaterials as advanced cancer therapeutics. *Small* **2019**, *15*, 1900172.
[171] Ouyang, C. H.; Zhang, S. B.; Xue, C.; Yu, X.; Xu, H.; Wang, Z. M.; Lu, Y.; Wu, Z. S. Precision-guided missile-like DNA nanostructure containing warhead and guidance control for aptamer-based targeted drug delivery into cancer cells *in vitro* and *in vivo*. *J. Am. Chem. Soc.* **2020**, *142*, 1265–1277.
[172] Yang, L.; Sun, H.; Liu, Y.; Hou, W. J.; Yang, Y.; Cai, R.; Cui, C.; Zhang, P. H.; Pan, X. S.; Li, X. W. et al. Self-assembled aptamer-grafted hyperbranched polymer nanocarrier for targeted and photoresponsive drug delivery. *Angew. Chem., Int. Ed.* **2018**, *57*, 17048–17052.
[173] Zhuang, X. X.; Ma, X. W.; Xue, X. D.; Jiang, Q.; Song, L. L.; Dai, L. R.; Zhang, C. Q.; Jin, S. B.; Yang, K. N.; Ding, B. Q. et al. A photosensitizer-loaded DNA origami nanosystem for photodynamic therapy. *ACS Nano* **2016**, *10*, 3486–3495.
[174] Wu, T. T.; Liu, J. B.; Liu, M. M.; Liu, S. L.; Zhao, S.; Tian, R.; Wei, D. S.; Liu, Y. Z.; Zhao, Y.; Xiao, H. H. et al. A nanobody-conjugated DNA nanoplatform for targeted platinum-drug delivery. *Angew. Chem., Int. Ed.* **2019**, *58*, 14224–14228.
[175] Ma, W. J.; Yang, Y. T.; Zhu, J. W.; Jia, W. Q.; Zhang, T.; Liu, Z. Q.; Chen, X. Y.; Lin, Y. F. Biomimetic nanoerythrosome-coated aptamer-DNA tetrahedron/maytansine conjugates: pH-responsive and targeted cytotoxicity for HER2-positive breast cancer. *Adv. Mater.*, in press, https://doi.org/10.1002/adma.202109609.
[176] Li, M. Y.; Wang, C. L.; Di, Z. H.; Li, H.; Zhang, J. F.; Xue, W. T.; Zhao, M. P.; Zhang, K.; Zhao, Y. L.; Li, L. L. Engineering multifunctional DNA hybrid nanospheres through coordination-driven self-assembly. *Angew. Chem., Int. Ed.* **2019**, *58*, 1350–1354.
[177] Chen, G.; Liu, D.; He, C. B.; Gannett, T. R.; Lin, W. B.; Weizmann, Y. Enzymatic synthesis of periodic DNA nanoribbons for intracellular pH sensing and gene silencing. *J. Am. Chem. Soc.* **2015**, *137*, 3844–3851.
[178] Liu, J. B.; Song, L. L.; Liu, S. L.; Jiang, Q.; Liu, Q.; Li, N.; Wang, Z. G.; Ding, B. Q. A DNA-based nanocarrier for efficient gene delivery and combined cancer therapy. *Nano Lett.* **2018**, *18*, 3328–3334.
[179] Liu, Q. L.; Bi, C.; Li, J. L.; Liu, X. J.; Peng, R. Z.; Jin, C.; Sun, Y.; Lyu, Y. F.; Liu, H.; Wang, H. J. et al. Generating giant membrane vesicles from live cells with preserved cellular properties. *Research (Wash D C)* **2019**, *2019*, 6523970.
[180] Luo, C.; Hu, X. X.; Peng, R. Z.; Huang, H. D.; Liu, Q. L.; Tan, W. H. Biomimetic carriers based on giant membrane vesicles for targeted drug delivery and photodynamic/photothermal synergistic therapy. *ACS Appl. Mater. Interfaces* **2019**, *11*, 43811–43819.